

# Evidence of Input From Lagged Cells in the Lateral Geniculate Nucleus to Simple Cells in Cortical Area 17 of the Cat

ALAN B. SAUL AND ALLEN L. HUMPHREY

*Departments of Neurobiology, Anatomy and Cell Science, University of Pittsburgh School of Medicine, Pittsburgh, Pennsylvania 15261*

## SUMMARY AND CONCLUSIONS

1. The visual cortex receives several types of afferents from the lateral geniculate nucleus (LGN) of the thalamus. In the cat, previous work studied the ON/OFF and X/Y distinctions, investigating their convergence and segregation in cortex. Here we pursue the lagged/nonlagged dichotomy as it applies to simple cells in area 17. Lagged and nonlagged cells in the A-layers of the LGN can be distinguished by the timing of their responses to sinusoidally luminance-modulated stimuli. We therefore used similar stimuli in cortex to search for signs of lagged and nonlagged inputs to cortical cells.

2. Line-weighting functions were obtained from 37 simple cells. A bar was presented at a series of positions across the receptive field, with the luminance of the bar modulated sinusoidally at a series of temporal frequencies. First harmonic response amplitude and phase values for each position were plotted as a function of temporal frequency. Linear regression on the phase versus temporal frequency data provided estimates of latency (slope) and absolute phase (intercept) for each receptive-field position tested. These two parameters were previously shown to distinguish between lagged and nonlagged LGN cells. Lagged cells generally have latencies >100 ms and absolute phase lags; nonlagged cells have latencies <100 ms and absolute phase leads. With the use of these criteria, we classified responses at discrete positions inside cortical receptive fields as lagged-like and nonlagged-like.

3. Both lagged-like and nonlagged-like responses were observed. The majority of cortical cells had only or nearly only nonlagged-like zones. In 15 of the 37 cells, however, the receptive field consisted of  $\geq 20\%$  lagged-like zones. For eight of these cells, lagged-like responses predominated.

4. The distribution of latency and absolute phase across the sample of cortical simple cell receptive fields resembled the distribution for LGN cells. The resemblance was especially striking when only cells in or adjacent to geniculate recipient layers were considered. Absolute phase lags were almost uniformly associated with long latencies. Absolute phase leads were generally associated with short latencies, although cortical cells responded with long latencies and absolute phase leads slightly more often than LGN cells.

5. Cells in which a high percentage of lagged-like responses were observed had a restricted laminar localization, with all but two being found in layer 4B or 5A. Cells with predominantly nonlagged-like responses were found in all layers.

6. Lagged-like zones can not be easily explained as a result of stimulating combinations of nonlagged inputs. Nonlagged-like responses could not be converted into lagged-like responses by increasing bar width.

7. We conclude that lagged and nonlagged geniculate inputs can be detected in the responses of cells in area 17. The influence of these inputs can be seen in the response timing at certain positions in the receptive field. Lagged afferents appear to innervate layer 4B.

## INTRODUCTION

It has been clear since the work of Hubel and Wiesel (1959, 1962) that the receptive-field properties of neurons in the primary visual cortex differ markedly from their afferents arising in the lateral geniculate nucleus (LGN). Nevertheless, there is evidence that classes of geniculocortical afferents are detectable at the cortical cell level, and some of them make obvious contributions to receptive-field properties. Perhaps the most striking example is the contribution of retinal and geniculate ON and OFF center cells to the spatially distinct ON and OFF zones of cortical simple cells, as revealed by silencing the ON pathway during application of D,L-2-amino-4-phosphonobutyric acid (APB) in the retina (Schiller 1982; Sherk and Horton 1984). Another method of obtaining evidence about the types of afferents influencing a cortical cell relies on electrical stimulation. Conduction speed and threshold differences between X- and Y-axons have permitted analysis of the extent to which single simple or complex cells (Hoffman and Stone 1971; Singer et al. 1975), in areas 17 or 18 (Stone and Dreher 1973; Ferster 1990), or in different cortical layers (Bullier and Henry 1979b; Ferster and Lindström 1983), receive inputs from each of these afferent streams. Some attempts have also been made at directly recording the inputs to cortical cells, with cross-correlation techniques (Lee et al. 1977; Tanaka 1983a, 1985; Toyama et al. 1977).

The primary method of characterizing the inputs to cortical cells has been simply to map receptive fields with extracellularly recorded responses to visual stimuli and then to associate the responses observed in cortex with characteristic response signatures of various types of LGN cells (Bullier et al. 1982; Citron et al. 1981; Ferster and Jagadeesh 1991; Mullikin et al. 1984; Tanaka 1983b). This is how Hubel and Wiesel (1962) first recognized the convergence of ON- and OFF-center afferents to simple cells. Although the results of such mapping studies are sometimes difficult to interpret, they can reveal the contribution of the geniculate inputs to cortical response properties. The most direct way of demonstrating inputs is through anatomic tracing (Davis and Sterling 1979; Ferster and LeVay 1978; Freund et al. 1985; Garey and Powell 1971; Humphrey et al. 1985; LeVay and Gilbert 1976), but establishing functional significance for labeled afferents is generally impossible.

The recently recognized population of lagged cells in the cat LGN provides a major projection to visual cortex (Humphrey and Weller 1988a; Mastronarde 1987a; Mastronarde et al. 1991). We have estimated that  $\sim 40\%$  of the X-relay cells are lagged ( $X_L$ ; Humphrey and Weller 1988b;

Mastrorade 1987a). None of the previous attempts to characterize thalamic inputs to visual cortex took into account this large lagged projection. We therefore wanted to investigate where these afferents to area 17 might terminate and what functions they might serve.

Unfortunately, tracing lagged cell axons into cortex has so far remained intractable, mainly because their small diameters preclude their impalement with micropipettes. Lacking good anatomic evidence, then, we undertook to examine single cortical neurons physiologically in search of signs of lagged inputs in their response properties. Lagged LGN cells are distinguished physiologically from their neighboring nonlagged cells on the basis of response timing (Saul and Humphrey 1990b). Sinusoidal luminance-modulation of a visual stimulus in time reveals these timing distinctions in terms of response phase behavior. Lagged cells fire about a quarter-cycle later than nonlagged cells of the same center-sign at low temporal frequencies. This timing difference is not due to a fixed delay, because it varies from 1 s at 0.25 Hz to 125 ms at 2 Hz, but instead reflects a tendency to respond to the removal of the appropriate luminance contrast. As temporal frequency increases, the response phase lag in lagged cells increases at a faster rate than is seen in nonlagged cells. By ~4 Hz, lagged and nonlagged cells of the same center-sign fire about a half-cycle apart. Lagged responses also have lower temporal resolution than nonlagged responses. Lagged and nonlagged cells have similar receptive-field size, center-surround interactions, and spatial resolution. Whereas X- and Y-cells differ prominently in spatial response properties but share temporal behavior (Derrington and Fuchs 1979; Lehmkuhle et al. 1980; Sestokas and Lehmkuhle 1986; Sherman 1985; Stone et al. 1979), lagged and nonlagged cells differ substantially only in their temporal properties (Saul and Humphrey 1990b).

To look for these distinctive response properties in cortex, we measured line-weighting functions with sinusoidally luminance-modulated bars at a series of positions across the receptive field. Values of response phase obtained at several temporal frequencies permitted comparisons of cortical response timing to the previous characterization of timing in the LGN. Although almost all the visual input to cortex is relayed through the lateral geniculate nucleus, cortical cells receive most of their inputs directly from other cortical neurons, and therefore do not behave like LGN cells. Nonetheless, cortical line-weighting functions revealed zones that closely resemble lagged and nonlagged geniculate afferents in their temporal response properties. These results constitute indirect evidence that lagged and nonlagged afferents provide inputs to cortical cells. In addition, this study provides further details about the spatiotemporal structure of visual cortical receptive fields.

Some aspects of this study have briefly appeared in abstract form (Saul and Humphrey 1990a).

## METHODS

Details of the physiological preparation are given elsewhere (Saul and Humphrey 1990b, 1992). Cats were prepared for single unit recording from visual cortex. Anesthesia was maintained during surgery with 1–1.5% halothane in nitrous oxide-oxygen

(70:30) and during recording with 0.1–0.5% halothane in the N<sub>2</sub>O-O<sub>2</sub> gas mixture. Heart rate, expired CO<sub>2</sub>, and the cortical electroencephalogram were monitored throughout the experiment. Single neurons were recorded extracellularly with glass micropipettes filled with 10% horseradish peroxidase (HRP) (Sigma) in 0.2 M KCl and tris(hydroxymethyl)aminomethane (Tris) buffer. We used these high-impedance electrodes (50–100 MΩ) to sample neurons with small as well as large somata (Humphrey and Weller 1988b; Mullikin et al. 1984).

For each cell the optimal orientation and minimal response field of the dominant eye were determined by hand plotting. Spatial and temporal frequency tuning curves in each direction were obtained with sinusoidal gratings presented on a Tektronix 608 monitor placed 57 cm from the eye. For all stimuli, mean luminance was 25 cd/m<sup>2</sup>, and contrast was ~40%. Stimulus timing and spike collection were accurate to 5 ms (limited by the 200-Hz frame rate). To look for lagged-like and nonlagged-like response timing, receptive-field structure was quantitatively determined from line-weighting functions generated by stationary bar stimuli whose luminance was modulated sinusoidally at various temporal frequencies (generally 0.5–8 Hz in octave steps). The bar was positioned at a series of locations spanning the receptive field. Bar width was nominally chosen to match the separation between adjacent positions (determined by the receptive-field width and the number of tested positions), but bar width was varied in some cases for comparison and to enable stronger responses. Typically, 0.3°-wide bars were used. The set of temporal frequency/bar position pairs was presented in random order, each trial lasting 4 s. The set was then repeated in a new random order, with a total of five iterations.

Responses were compiled into histograms representing the average firing rate during each stimulus cycle for each trial. Bin-widths were ~8 ms. Means and standard errors over the five trials for each stimulus condition were computed, with the first harmonic component of the response. Standard errors for phase were computed in the complex plane, with deviations weighted by the amplitudes. Simple and complex cells were distinguished on the basis of the segregation of ON and OFF zones in hand plots and in the quantitatively obtained line-weighting functions, as well as larger first harmonic than direct current response amplitude when tested with drifting gratings (De Valois et al. 1982).

For each temporal frequency, response amplitude and phase were plotted against spatial position. Response phase was measured in cycles, with a value of 0.0 cycles corresponding to an ON-response that is in register with the luminance peak and a value of 0.5 cycles corresponding to an OFF-response that is in register with the luminance trough (Saul and Humphrey 1990b). A response that leads the stimulus has a phase value between -0.25 and 0 cycles or between 0.25 and 0.5 cycles. Phase lags have values in the other quarter-cycles, either between 0.0 and 0.25 cycles or between 0.5 and 0.75 cycles (Table 1). Because phase values can be placed in any cycle by addition or subtraction of any integer, they were adjusted so that points representing neighboring receptive-field positions were less than a half-cycle apart, and so that phase increased with temporal frequency (see Figs. 4 and 7). When these conditions conflicted (because of weak response amplitudes that sometimes produced unreliable phase values), values were adjusted by hand to maximize consistency with the most responsive positions.

The response amplitude and phase values were then replotted as functions of temporal frequency for each position. Lines were fit to the phase versus temporal frequency data. For these fits, the data were weighted by the reciprocals of the standard errors of the response phase means and by the square roots of the mean response amplitudes. These fits provided two parameters: the intercept, which we refer to as *absolute phase*; and the slope, which we call *latency*. Estimates of standard deviations for these parameters

TABLE 1. Absolute phase ranges for different response types

	Cycles	
	ON	OFF
Nonlagged	-0.25-0.0	0.25-0.5
Lagged	0.0-0.25	0.5-0.75

were also available, as were values of the goodness-of-fit and regression coefficient. We rejected data if the standard deviation of absolute phase exceeded 0.1 cycles, the standard deviation of latency exceeded 40 ms or 25% of the latency, the latency was <30 ms or >300 ms, or the regression coefficient was <0.4. Goodness-of-fit, which in principle should provide a criterion for rejecting or accepting the fitted parameters, was low (below 0.1) in many cases even though the data were fairly linear, because the standard errors of our phase measurements were typically vanishing when responses were at all vigorous (and goodness-of-fit was often near 1.0 when responses were weak because the standard errors were sizable).

We marked the end of a penetration by ejecting HRP from the electrode tip. At the end of the experiment the animal was killed with an intravenous injection of Nembutal (Abbott Labs) and perfused transcardially with 1% paraformaldehyde and 2% glutaraldehyde. The brain was blocked in the plane of the penetrations, cut at 50 or 100  $\mu\text{m}$ , reacted to reveal the HRP, and counterstained with cresyl violet. Electrode tracks were reconstructed and laminar positions of recording sites were estimated with criteria described in Humphrey et al. (1985).

RESULTS

Response phase characteristics

Previous work showed that lagged and nonlagged cells in the cat LGN can be distinguished by presenting stationary spots in the receptive field, modulating their luminance sinusoidally at a series of temporal frequencies, and measuring response phase (Saul and Humphrey 1990b). We repeated these experiments on a sample of cortical neurons, with the necessary modifications of using appropriately oriented bars presented at a series of positions across the receptive field. In this section we first illustrate the data analysis techniques for two isolated receptive-field positions in a simple cell. We then present this analysis in the context of the entire receptive field. Finally, the results compiled from the entire sample of 37 area 17 simple cells are presented. All of these cells had receptive fields within  $10^\circ$  of the area centralis.

Data from a direction selective simple cell in layer 5A are illustrated in Fig. 1. Responses obtained at 2 of the 21 positions tested in this cell's receptive field are illustrated for five of the seven tested temporal frequencies. These two positions are indicated in the handplotted receptive field shown in the figure inset. They were located on each side of the handplotted central OFF zone, near but not inside the ON flanks. Response histograms averaged over one cycle of the visual stimulus are shown with the cycle repeated for clarity. The response phase ( $\phi$ ), measured in cycles, is indicated above each histogram. As in the LGN (cf. Saul and Humphrey 1990b; Fig. 6), two patterns of timing emerge. The zone illustrated on the left responds in the manner of OFF-center nonlagged geniculate cells, with a phase lead (phase values <0.5 cycles) at low temporal frequencies and

a relatively slow increase in response phase with frequency. In contrast, the zone shown on the right has responses that resemble those of OFF-center lagged geniculate neurons, characterized by a phase lag (>0.5 cycles) at low frequencies and a high rate of increase of phase with frequency. Note that the phase difference between these two zones approximates a quarter-cycle at 1 Hz but increases to more than a half-cycle by 4 Hz. At 4 Hz, the responses of the zone at  $0^\circ$  are much weaker than at lower frequencies, but the timing is nonetheless clear and reliable. At 0.5 Hz, on the other hand, the response of this zone is weak and the phase value is less reliable.

To quantify such responses, we performed the analysis used in the LGN, plotting response phase versus temporal frequency (Saul and Humphrey 1990b). Data from the two positions used for Fig. 1 are shown in Fig. 2. As observed

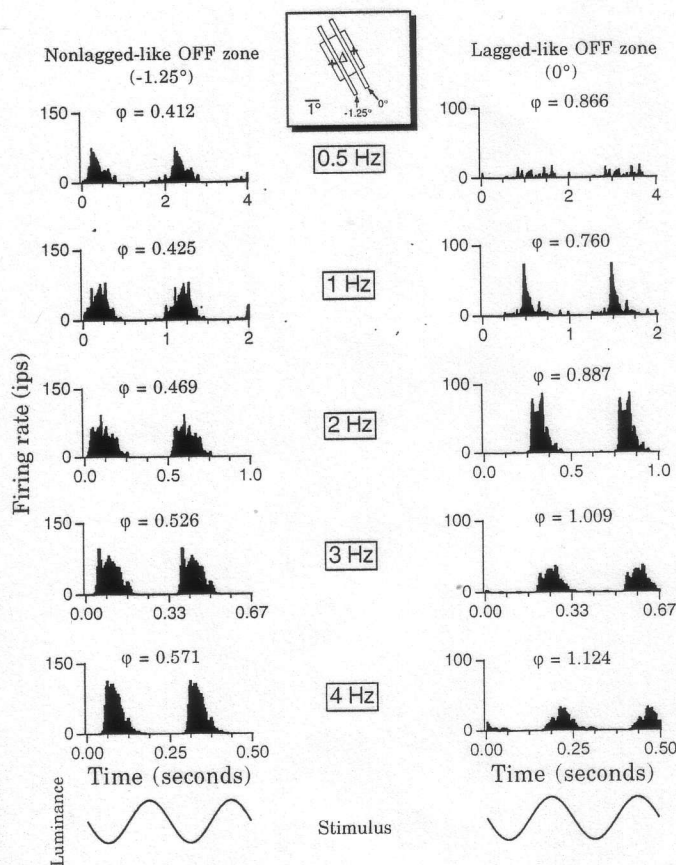


FIG. 1. Response histograms are shown for 2 of 21 tested positions and 5 of 7 tested temporal frequencies from a layer 5A direction selective simple cell. The stimulus consisted of sinusoidal luminance-modulation of a  $0.3 \times 6^\circ$  bar. Two cycles are shown for clarity. The sine waves below the histograms describe the luminance waveform; note that the bar darkened initially, so that responses occurring early in the cycle at low temporal frequencies represent OFF responses. Five 8-s trials were obtained for each of the 147 conditions (7 temporal frequencies times 21 positions). The mean first harmonic phase values over these 5 trials are given above each histogram, in cycles relative to the stimulus luminance. An integer number of cycles can be added or subtracted to any phase value, so that for instance 0.887 cycles is the same as -0.113 cycles, and 1.124 cycles is the same as 0.124 cycles. However, because responses occur later in the stimulus cycle as temporal frequency increases, we choose phase values that increase with temporal frequency, as shown here. The inset at the top diagrams the hand-plotted receptive field, with bars at the same scale placed to represent the illustrated test positions.

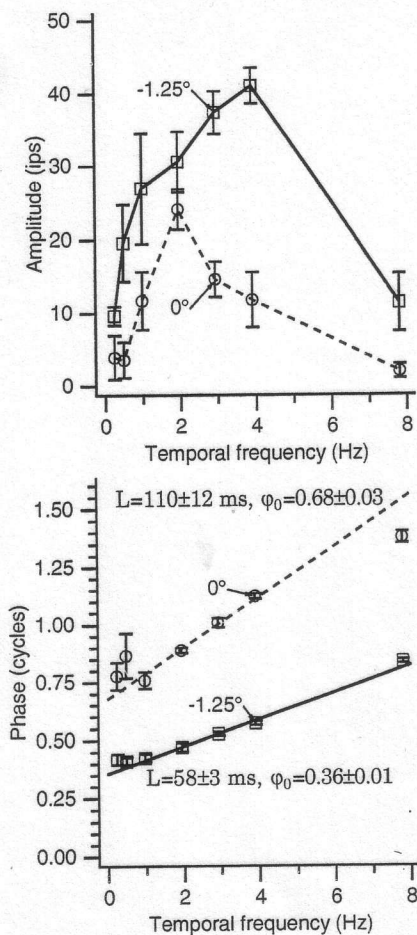


FIG. 2. First harmonic amplitude and phase values from the receptive field positions illustrated in Fig. 1 are plotted against the full range of tested temporal frequencies. Points represent means and standard errors over 5 trials; square symbols represent data from the position at  $-1.25^\circ$ , and circles from  $0^\circ$ . Regression lines through the phase values are shown as well, and the latency ( $L$ ) and absolute phase ( $\phi_0$ ) values are given. These are, respectively, the slopes and intercepts of the lines, and are given as means  $\pm$  standard deviations. Note that the weak amplitudes and unreliable phase values at 0.25 and 0.5 Hz for the zone at  $0^\circ$  cause these points to contribute relatively little to the weighted linear regression, and the linearity of the points between 1 and 4 Hz can be seen.

previously (Hamilton et al. 1989; Lee et al. 1981; Reid et al. 1992; Saul and Humphrey 1990b) the phase versus temporal frequency points plotted in Fig. 2 are fit reasonably well by straight lines. The best-fitting lines through the phase data from these two positions are illustrated by the solid and dashed lines through the square and circle symbols, respectively. Linear regression yields two parameters, a slope and an intercept. These two parameters distinguish between lagged and nonlagged geniculate neurons (Saul and Humphrey 1990b). The intercepts indicate the response phase extrapolated to 0 Hz, which we refer to as "absolute phase." This parameter provided the key to understanding the visual response profiles of lagged and nonlagged geniculate cells. In general, nonlagged cells have absolute phase leads, whereas lagged cells have absolute phase lags. The second parameter from the linear regressions is the slope, which we call "latency" and others refer to as "integration time" (Hamilton et al. 1989; Reid et al. 1992). Lagged cells in the LGN have longer latencies than nonlagged cells when measured in this way. Most nonlagged

cells have latencies  $< 100$  ms and most lagged cells have latencies  $> 100$  ms. The latencies and absolute phase values from the cortical cell in Fig. 2 are 58 ms and 0.358 cycles for the zone at  $-1.25^\circ$  and 110 ms and 0.678 cycles for the

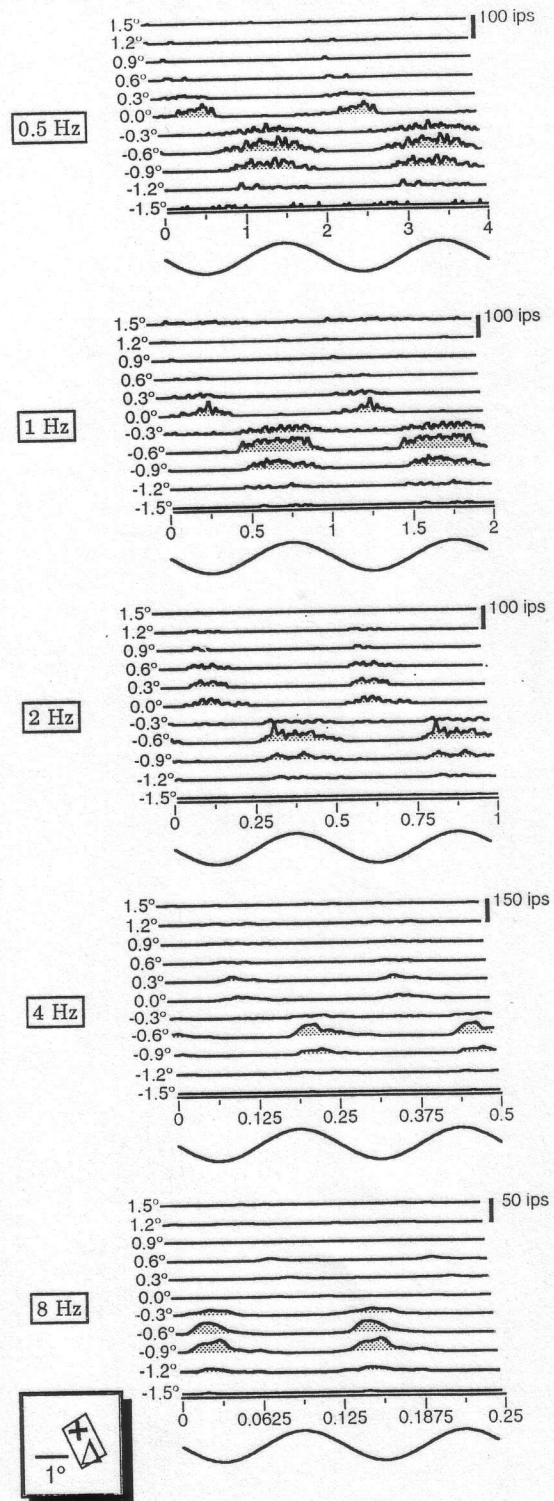


FIG. 3. Histograms are plotted for all 11 positions and 5 temporal frequencies tested in a simple cell recorded near the layer 3/4 border. The stimulus was a  $0.3 \times 8^\circ$  bar. The positions labeled  $-1.5$  and  $1.5^\circ$  were beyond the top and bottom, respectively, of the receptive field illustrated in the inset. Note that response amplitude scaling changes with temporal frequency; the vertical scale is indicated by the calibration bar at the top right of each set of histograms.

zone at  $0^\circ$ . Because of the similarities of these cortical cell response patterns to the behavior of lagged and nonlagged geniculate cells, we label them as nonlagged-like and lagged-like, respectively. Henceforth, we will use the term "lagged-like" to refer to receptive-field positions that reliably show absolute phase lags and latencies  $>100$  ms and "nonlagged-like" for absolute phase leads and latencies  $<100$  ms. Table 1 summarizes the absolute phase values for each of these classifications (see Fig. 14 as well).

#### Examples of cortical receptive fields

The complete experimental design is illustrated with the example in Figs. 3–5, from a simple cell located in layer 4A. This cell was tested with a  $0.3 \times 8^\circ$  bar at 11 positions over  $3^\circ$  and at 5 temporal frequencies. Histograms for each position and temporal frequency are shown in Fig. 3. Two cycles are shown for clarity. There are two main zones, a strong ON region around  $-0.6^\circ$  and a weaker OFF region around  $0.3^\circ$ . At 0.5 Hz, the ON responses occur mainly as luminance increases, and the OFF responses as luminance decreases. Responses generally peak before the peak or trough of the luminance: the responses lead the stimulus. At 2 Hz the responses occur close to the luminance peak or trough, and at 4 or 8 Hz the responses occur after them.

The first harmonic amplitudes and phases for these 55 points are plotted in Fig. 4 to provide line-weighting functions. The scaling is maintained across all temporal frequencies here and is given for the 0.5-Hz graphs. The horizontal axis indicates receptive-field position. The markers

with error bars show the means and standard errors over the five trials for each condition. The structure of the receptive field is shown clearly by the half-cycle jump in response phase between the ON and OFF zones and by the bimodal amplitude curves at 2 and 4 Hz. The ON zone has been plotted here a half-cycle later than the OFF zone but could have been shifted down one cycle so that it would appear a half-cycle earlier than the OFF zone. Note that even where response amplitudes are low, such as at  $0.6^\circ$ , phase values are fairly reliable (except at 0.5 and 8 Hz) and consistent with their neighboring positions. Only when responses practically vanish do phase values become unreliable, as at  $-1.5$  or  $1.5^\circ$ . The high reliability of the phase measurements suggests that response timing serves important functions in neuronal processing.

These data were also plotted against temporal frequency, and latency and absolute phase values were computed for each position. Figure 5 shows these results for positions that gave adequate responses. Criteria for defining adequate responses are described in METHODS, with the use of estimates of the standard deviations of latency and absolute phase that were in turn based on the standard errors of the individual phase points and on the corresponding amplitudes. Four of the 11 positions tested in this cell were rejected by these criteria. For the remaining seven positions, the absolute phase values were between 0.40 and 0.46 cycles for the OFF zone and between 0.86 and 0.93 cycles for the ON zone. The latencies ranged from 65 to 76 ms. These absolute phase and latency values are in the nonlagged ranges for the LGN.

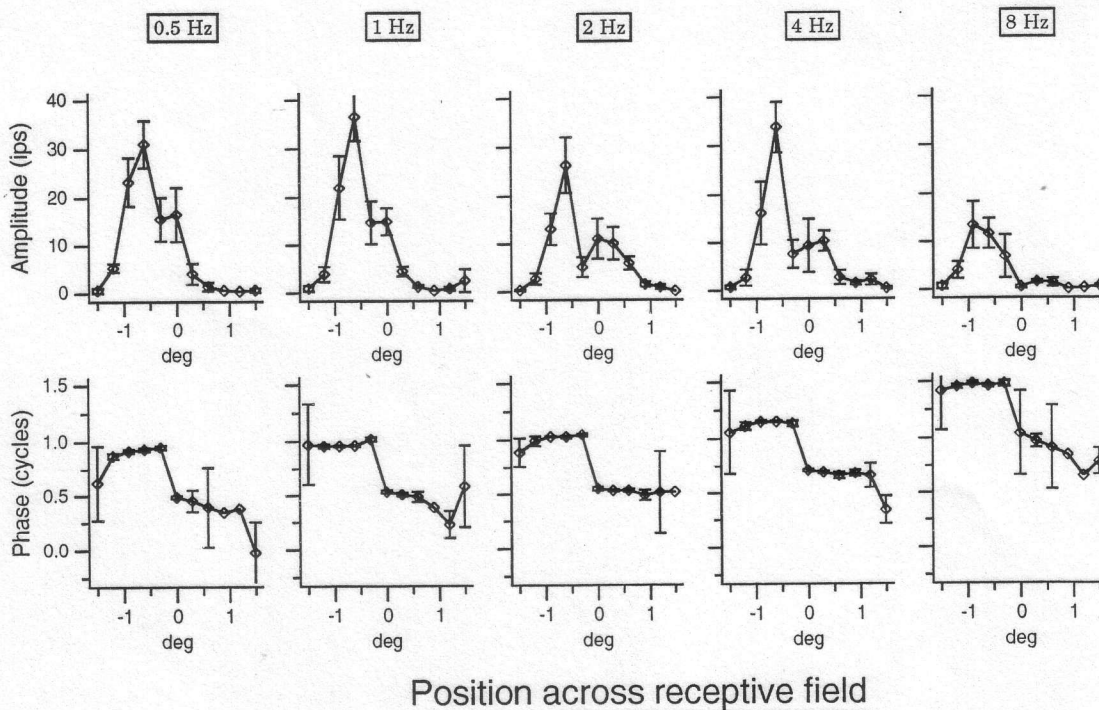


FIG. 4. Line-weighting functions from data used to generate Fig. 3. First harmonic amplitude and phase are plotted as functions of position for each temporal frequency. Means and standard errors are shown. For many of the phase means, the standard errors are too small to be visible here. For a few points, not enough spikes were present to obtain standard errors, and thus no error bars are shown. Phase values were adjusted by addition of integers to minimize the difference between adjacent positions and maintain increasing phase with temporal frequency. In this case for instance, because phase is practically constant except for a half-cycle jump between  $-0.3$  and  $0.0^\circ$ , the differences between adjacent positions would have been only slightly increased had 1 cycle been subtracted from the values at  $-1.5^\circ$  through  $-0.3^\circ$ .

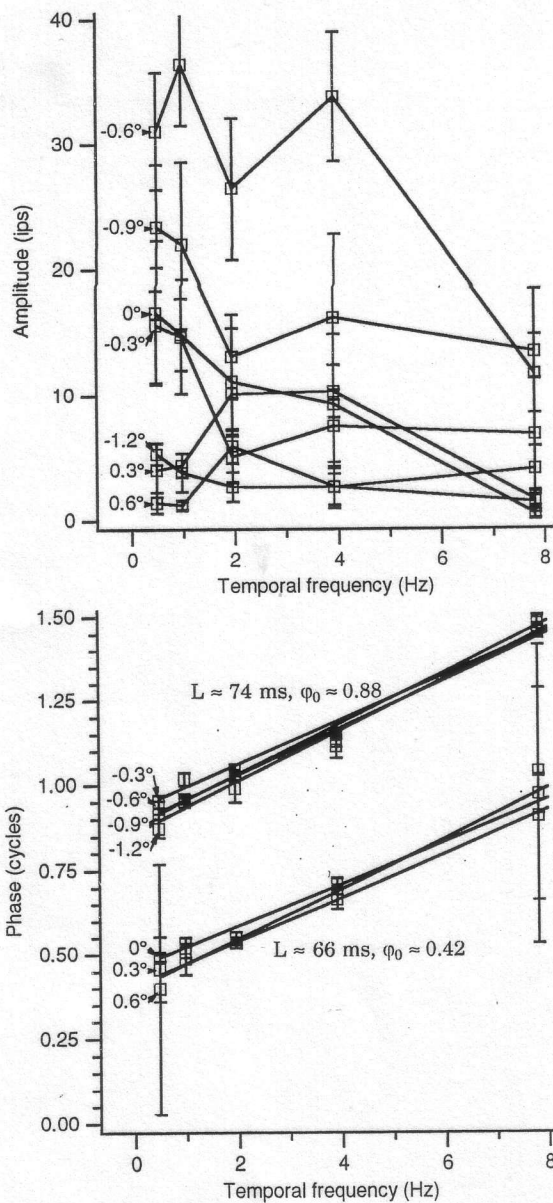


FIG. 5. The data in Fig. 4 showing amplitude and phase as a function of space for each temporal frequency are replotted as functions of temporal frequency for each position. Only 7 of the 11 tested positions are illustrated here. The regression lines illustrated here all had slopes ( $L$ ) and intercepts ( $\varphi_0$ ) with small standard deviations. Latencies ranged from 70–76 ms for the ON region ( $-1.2$  to  $-0.3^\circ$ ) and 65–74 ms for the OFF region (0.0 to  $0.6^\circ$ ). Absolute phase values ranged from 0.858–0.928 (equivalent to  $-0.142$  to  $-0.072$ ) cycles for the ON region and 0.399–0.462 cycles for the OFF region. Note the reliability of the phase data and the variability of the amplitude data. For abbreviations, see Fig. 2 legend.

This type of simple cell receptive field is called spatiotemporally separable (Adelson and Bergen 1985; McLean and Palmer 1989; Reid et al. 1987, 1991). The receptive field can be modeled as a product of two functions, one of which depends only on spatial position and the other only on time. A separable field has response phase values that are constant or that differ by multiples of a half-cycle as a function of space. Almost all early studies of receptive-field structure relied on classifying responses as ON or OFF, presumably because these classifications are based on what was then known about the geniculate afferents (Hubel and Wiesel 1961). Implicit in this view of cortical receptive fields is

an assumption of separability, that responses can be put in just two phase classes (ON and OFF) a half-cycle apart.

As has been reported previously (Albrecht and Geisler 1991; Dean and Tolhurst 1986; McLean and Palmer 1989;

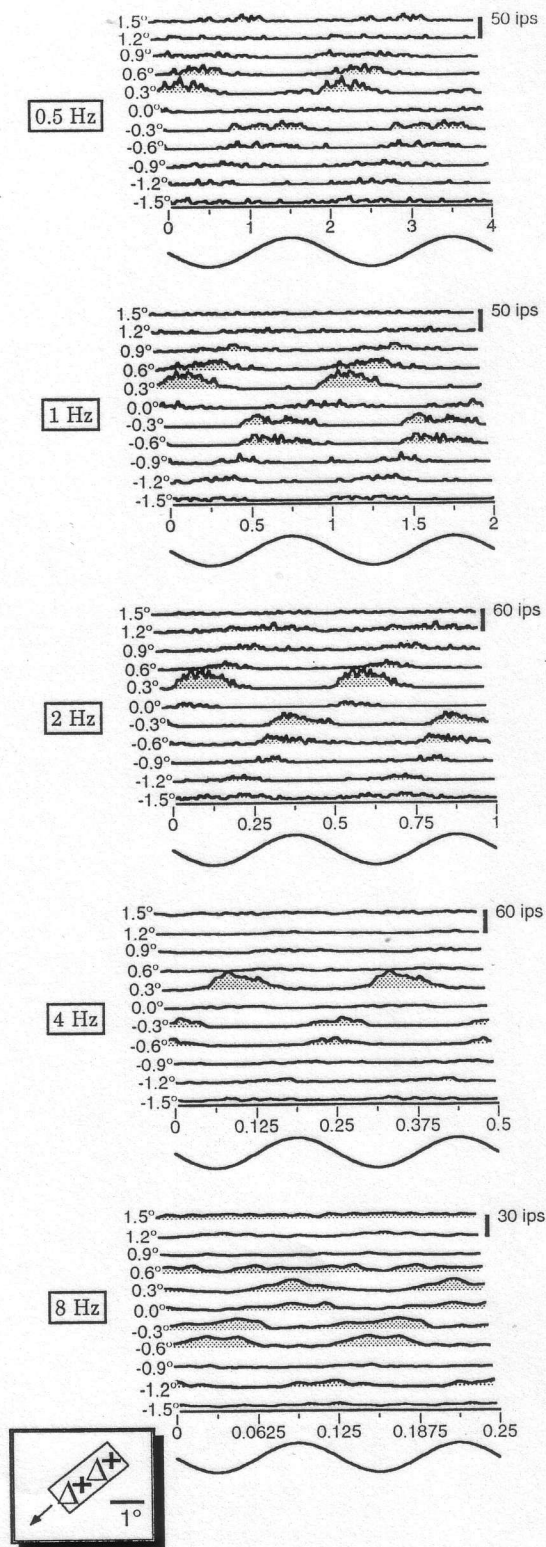


FIG. 6. Histograms from a direction selective cell in layer 5A, in the same format as Fig. 3. These data were obtained by testing with a  $0.5 \times 7^\circ$  bar. The position labeled  $-1.5^\circ$  was located at the lower left edge of the schematic receptive field and the position labeled  $1.5^\circ$  was at the top right.

Movshon et al. 1978; Reid et al. 1987, 1988, 1991; Tolhurst and Dean 1991), some simple cells have not only classical ON and OFF zones but also zones that are intermediate in their response timing. Most cells are in fact inseparable, having response timing that varies more gradually with position. An example of line-weighting function data from such a cell is given in Figs. 6 and 7. This layer 5A cell was direction selective at low temporal frequencies. Eleven positions  $\geq 3^\circ$  were tested with a  $0.5 \times 7^\circ$  bar, at five temporal frequencies.

This cell had clear ON and OFF zones, but response timing varied smoothly across the receptive field, as seen by the bottom left to top right slant of the responses in Fig. 6. Response phase varies smoothly in Fig. 7, at least at low temporal frequencies, instead of jumping by a half-cycle as in Fig. 4. Whereas in Fig. 4 the phase values could have reasonably been plotted as either increasing or decreasing with position, here there is no question that phase increases across the receptive field. This difference between separable and inseparable cells correlates with their direction selectivity. Separable cells tend to respond to both directions of stimulus movement, whereas inseparable cells respond only or primarily to the direction in which phase decreases in these plots (Albrecht and Geisler 1991; McLean and Palmer 1989; Reid et al. 1987, 1991; Saul and Humphrey 1990a; Tolhurst and Dean 1991).

For six of the receptive-field positions, we replot the responses against temporal frequency in Fig. 8. The lines fit to the phase versus temporal frequency data provide the latency and absolute phase values listed in parentheses on the figure. The six positions illustrated in Fig. 8 alternate in their phase behavior, with nonlagged-like timing at  $-1.2$ ,  $-0.3$ , and  $0.3^\circ$  (—) and lagged-like timing at  $-0.9$ ,  $0$ , and  $0.9^\circ$  (---). The responses at  $-0.6$  and  $0.6^\circ$  were also non-

lagged-like, and at  $1.2^\circ$  they were lagged-like; for clarity, these positions were not shown. This cell's ON and OFF zones could thus be subdivided into lagged-like and nonlagged-like regions. The hand-plotted ON zone at the top of the receptive field in Fig. 6 actually turned out to be a lagged-like OFF zone (this is a common confusion when hand-plotting lagged LGN cells).

#### Controls for potential artifacts

To interpret these cortical responses in terms of separately recorded geniculate data, their stability and independence from interactions between inputs must be demonstrated. When possible, line-weighting functions were obtained repeatedly to demonstrate stability. Figure 9 shows data obtained immediately after the run that produced the data in Figs. 6–8. In this run, bar width was reduced to  $0.2^\circ$ , and the response amplitudes were weaker and more variable because of this narrower stimulus. However, the lagged-like zones did not disappear, indicating that they were not an artifact of the wider bar used earlier. The receptive field structure revealed in Fig. 9 is similar to that in Fig. 8, with alternation between nonlagged-like and lagged-like zones. The large variability of some of the latency and absolute phase values (e.g., at  $0.3$  and  $-1.2^\circ$ ) would lead to their rejection by our criteria, but they are listed here solely for comparison to Fig. 8. The latencies at  $0.3$  and  $-1.2^\circ$  become  $111 \pm 12$  and  $117 \pm 45$  (SD) ms, respectively, but the large standard deviations associated with these values render them not significantly different from those obtained in the previous run ( $91 \pm 5$  and  $93 \pm 10$  ms, respectively).

An argument can be advanced that lagged-like zones appear between adjacent nonlagged-like zones when the test bar activates an ON and an OFF zone simultaneously. Al-

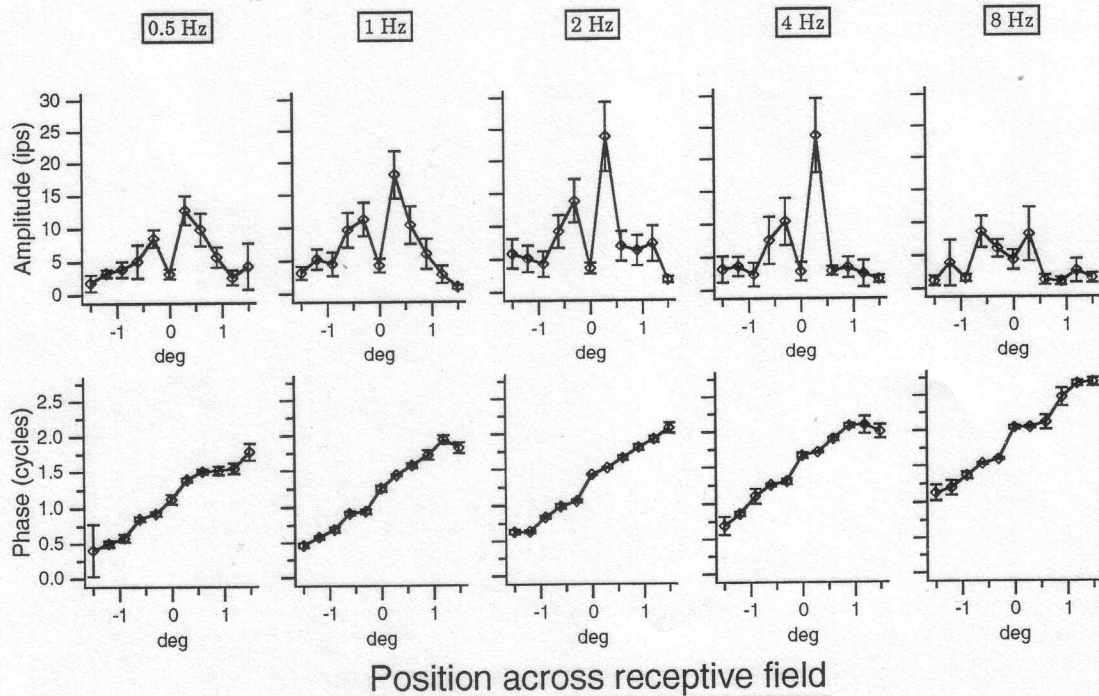


FIG. 7. Line-weighting functions for the cell illustrated in Fig. 6, presented in the same format as Fig. 4. In this case there is a natural choice of the cycle in which to place phase values, because phase varies in small steps from one position to the next, at least at low temporal frequencies.

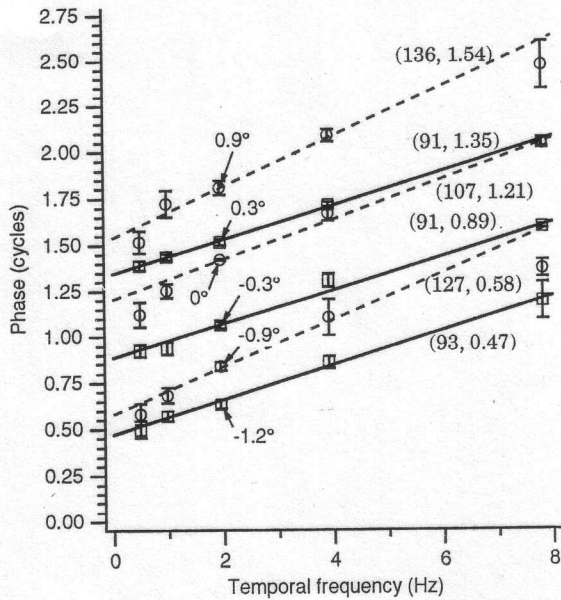
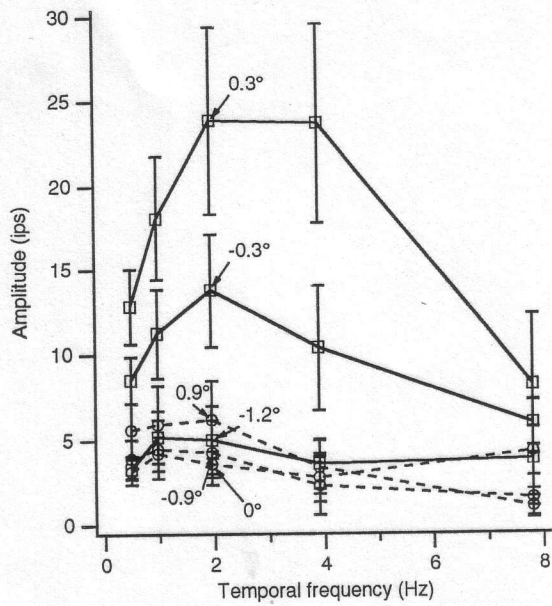


FIG. 8. Data from 6 of the positions in Figs. 6 and 7 are plotted against temporal frequency, following the format of Fig. 5. The latencies (in milliseconds) and absolute phase values (in cycles) for these positions are listed in parentheses. Positions giving long latencies and absolute phase lags (lagged-like responses) are shown with dashed lines and circles; nonlagged-like positions are shown with solid lines and squares. The absolute phase values at  $-0.3$ ,  $0$ ,  $0.3$ , and  $0.9^\circ$  are equivalent to  $-0.11$ ,  $0.21$ ,  $0.35$ , and  $0.54$  cycles, respectively. The ordering of these positions with phase increasing across the receptive field is maintained this way. Positions at  $-1.2$ ,  $-0.9$ ,  $0.3$ , and  $0.9^\circ$  gave OFF responses, and  $-0.3$  and  $0^\circ$  gave ON responses.

though this would be difficult to achieve in principle (see DISCUSSION), an empirical control is to test separable receptive fields with wide bars to try to produce lagged-like zones at these borders. An example of such a test is shown in Fig. 10, for a cell at the layer 5/6 border that had an ON zone flanked by OFF zones. Line-weighting functions were obtained at 11 positions over  $2^\circ$  at 3 temporal frequencies in consecutive runs with bars that were  $3^\circ$  long and  $0.1$ ,  $0.2$ , and  $0.5^\circ$  wide. For simplicity only the  $0.5$ -Hz histograms are shown for the  $0.2$  and  $0.5^\circ$  bar widths, but these results are representative of the other temporal frequencies, with

the  $0.1^\circ$ -wide bar giving responses like the  $0.2^\circ$ -wide bar but somewhat weaker. Latencies and absolute phase values for the ON zone were  $\sim 80$  ms and  $-0.04$  cycles. Responses were too weak in the OFF flanks to provide reliable phase data. The  $0.5^\circ$ -wide bar allowed the OFF-flanks to be revealed more clearly (compare error bars in the phase plots), but did not induce any lagged-like responses at the borders between the ON and the OFF zones. Instead, when the widest bar was positioned at  $0.2^\circ$  and stimulated both the central

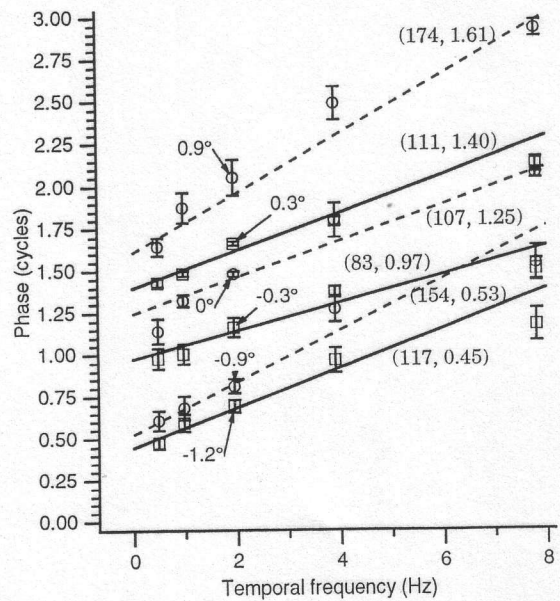
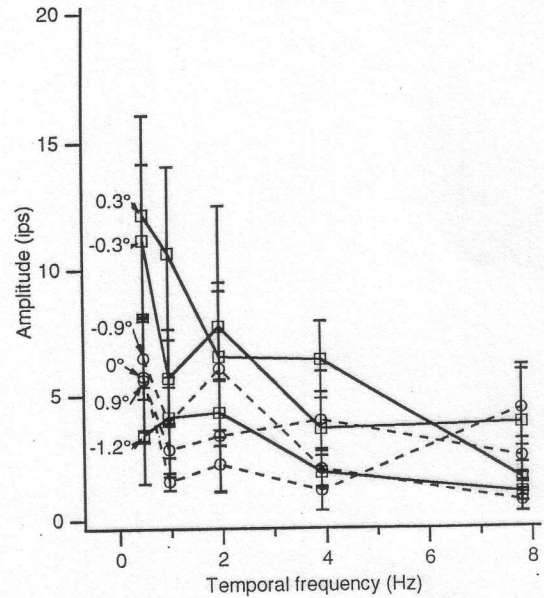


FIG. 9. Responses from another run following that shown in Figs. 6–8 are plotted against temporal frequency. This experiment was identical to the preceding one except that the bar width was reduced to  $0.2^\circ$ . Response amplitudes were lower and more variable and the reliability of the phase values was lower because the narrower bar was a less effective stimulus. However, the same picture of the receptive field structure can be seen, with lagged-like (---) and nonlagged-like zones (—) alternating. Latency and absolute phase values are given in parentheses, despite several of these values (at  $-1.2$  and  $-0.9^\circ$ ) being unreliable according to our criteria. None of these derived measurements differs significantly from those found in the preceding run, listed in Fig. 8. More importantly, the actual phase data points are almost identical between the 2 runs wherever responses were reliable.

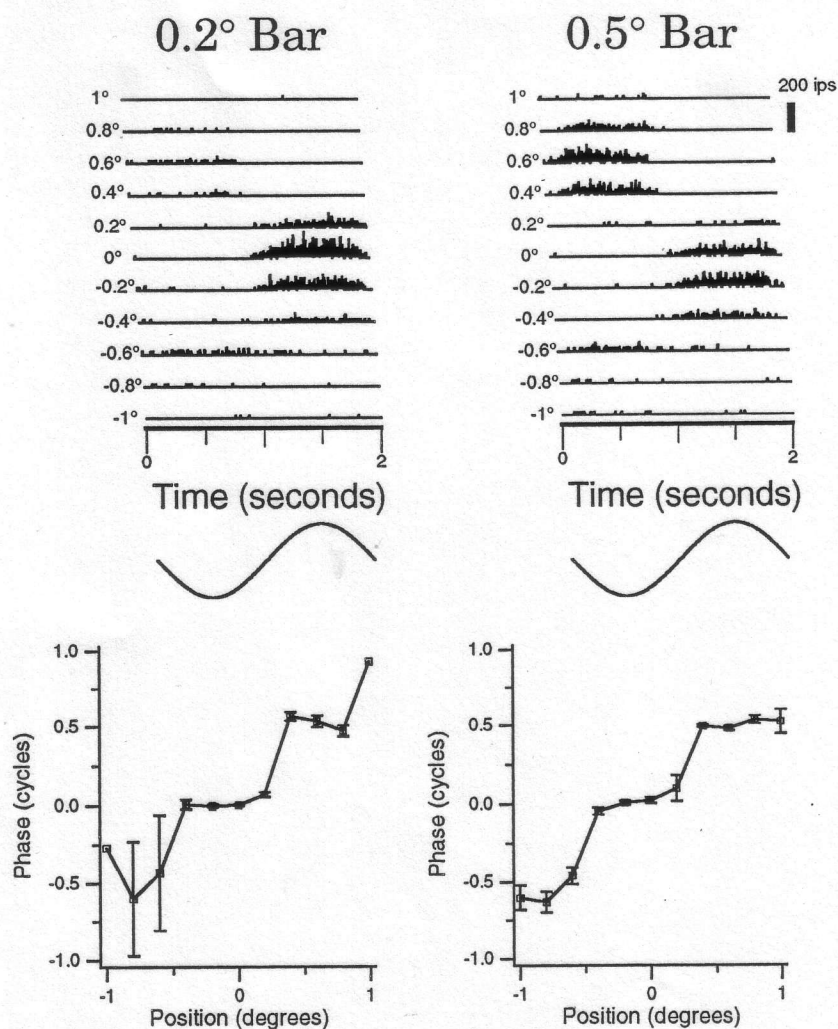


FIG. 10. Histograms from a layer 5/6 border cell are shown for 1 of the 3 tested temporal frequencies and for 2 bar widths. The corresponding phase values are shown below each set of histograms. Data for each bar width were collected in consecutive but separate, noninterleaved experiments. The 200 imp/s scale bar applies to all histograms. This cell was separable and showed only nonlagged-type responses. When the 0.5°-wide bar was positioned at 0.2°, it stimulated both the central ON region and the neighboring OFF region. As a result, the small ON response elicited from this position with the 0.2°-wide bar was greatly diminished, and the phase value was less reliable. No lagged-like responses were induced by testing with the 0.5°-wide bar.

ON zone and the neighboring OFF flank, the small ON response evident with the narrower bars was suppressed. Thus, reliable latency and absolute phase values could not be obtained at the border, but latencies in the ON zone were slightly increased to  $\sim 90$  ms, and absolute phase remained  $\sim -0.04$  cycles. As seen in the plots of phase versus position, the receptive field remained separable when tested with the wider bar. Multiple line-weighting functions, with bars of varying width, were obtained from three other cells. Wider bars generally improved responses when they were centered over a similarly wide zone, but led to reductions of responsiveness where they encroached on zones of opposite polarity. In no case did they induce responses with lagged-type timing from positions that had nonlagged-type timing, when tested with narrower bars. Most line-weighting functions were obtained with reasonably wide bars (generally 0.3–0.5°) to elicit adequate responses, however.

Could lagged-like responses be an artifact of weak responsiveness, perhaps because of cortical filtering? Response amplitudes of lagged-like zones tended to be weaker than nonlagged-like zones in general. This is illustrated in Figs. 2 and 8. Another example is shown in Fig. 11, from a layer 6 cell. Most of the positions tested showed nonlagged-like timing, but ON-center lagged-like timing was observed at one position ( $-0.2^\circ$ ) between ON and OFF nonlagged-like zones. The lagged-like responses at  $-0.2^\circ$  were of similar

amplitude to the nonlagged-like responses at  $0^\circ$  when tested at 0.5 Hz, but remained  $<10$  imp/s at 1–4 Hz, whereas the responses at  $0^\circ$  grew to a peak of  $\sim 20$  imp/s at 4 Hz. This might suggest that the difference between lagged-like and nonlagged-like responses could be the result of low-pass filtering. Although low-pass filtering could be an important component of lagged-like responses, by itself it does not account for the phase behavior of these zones at low temporal frequencies, as discussed further below. In fact, the correlation between lagged-like phase behavior and low-pass tuning was not strict. The other nonlagged-like positions shown in Fig. 11 have amplitudes similar to the lagged-like position. Furthermore, as shown below (Fig. 12), lagged-like zones were sometimes tuned to higher temporal frequencies. The response amplitude differences between lagged-like and nonlagged-like positions in simple cells may reflect the hypothesized geniculate inputs. In the LGN, response amplitudes tend to be lower in lagged cells than in nonlagged cells (Humphrey and Weller 1988a; Mastronarde 1987a; Saul and Humphrey 1990b), and  $X_L$ -cells are tuned to slightly lower temporal frequencies than nonlagged X ( $X_N$ )-cells (Saul and Humphrey 1990b).

In cortex, the difference in response amplitude between the lagged-like and nonlagged-like zones sometimes appeared to be exaggerated relative to the LGN, as seen in Fig. 8. In cells that had both types of timing, nonlagged-like

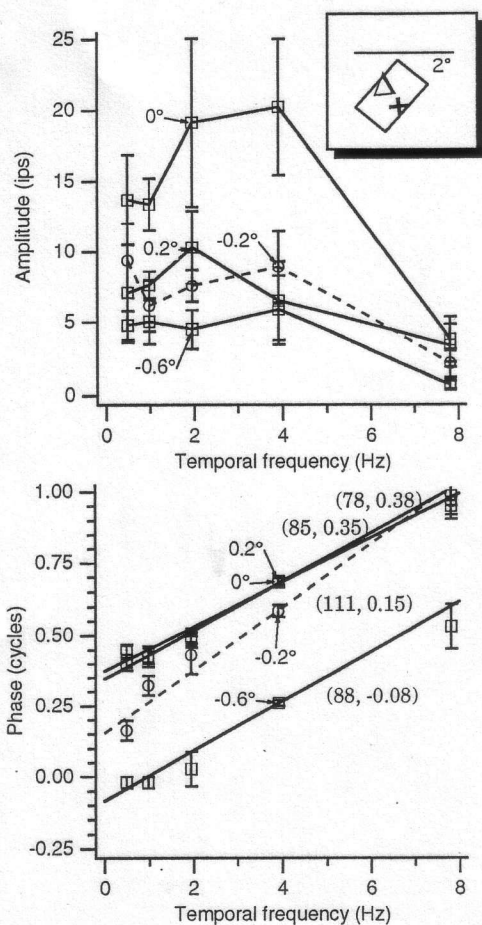


FIG. 11. Responses at 4 positions in a layer 6 cell are plotted against temporal frequency. This cell was tested with a  $0.3 \times 6^\circ$  bar at 11 positions and 5 temporal frequencies. The ON responses seen at  $-0.6^\circ$  arose from the hand-plotted ON zone at the bottom right of the diagram in the inset, with the other plotted responses coming from the hand-plotted OFF zone. The lagged-like responses at  $-0.2^\circ$  are shown with dashed lines and circles. Latencies and absolute phase values are listed in parentheses.

response amplitudes sometimes dwarfed lagged-like amplitudes. The apparent low-response amplitudes associated with lagged-like cortical zones present a potential problem in interpretation, because weak responses tend to be less reliable, and the lagged-like phase values might be due to this variability. This was not the case, however. Besides the precautions taken to reject unreliable data, there were cells in which strong response amplitudes were associated with lagged-like response timings. An example is shown in Fig. 12. The entire main response region (running from the hand-plotted ON zone at  $\sim -2^\circ$  to the OFF zone at  $\sim -0.5^\circ$ ) had lagged-like ON responses. The plot of phase versus temporal frequency in Fig. 12B demonstrates the consistency of the lagged-type responses, with their intercepts  $\sim 0.1$  cycles and slopes  $> 100$  ms. The weak nonlagged-like OFF zone can be seen above the main zone (at  $0^\circ$ ). Thus, weak responses in themselves do not imply lagged-like timings.

The reliability of the phase measurements made it possible to specify whether responses were lagged-like or nonlagged-like even when responses were weak, as is apparent from the lagged-like zones in Fig. 8 or the nonlagged-like zone in Fig. 12, as well as in Fig. 13, where results from a layer 6 cell are shown. This cell was tested at 21 positions with a  $0.5 \times 4^\circ$  bar modulated at seven temporal frequen-

cies. The receptive field structure was clearly revealed by these tests, showing separate ON and OFF zones, but responses were uniformly poor across the receptive field. The weak activity recorded in this cell revealed consistent nonlagged-like phase values, with none of the 21 positions tested giving lagged-like responses. Plotted in Fig. 13 are data from the most responsive position in each zone. Mean amplitudes were all  $< 10$  imp/s and were noisy and poorly tuned as a function of temporal frequency. The phase values were nonetheless consistent from one position to the next (as in Fig. 5), showing absolute phase leads and latencies  $< 100$  ms. Thus, there was not a strong correlation between amplitude and phase characteristics, and lagged-like timing was not an artifact of poor responsiveness. In fact, the response amplitude difference between lagged-like and nonlagged-like zones was smaller than the corresponding difference in the LGN. The average first harmonic response amplitude at the best temporal frequency was  $11 \pm 7$  spikes/s for 37 lagged-like zones and  $13 \pm 9$  spikes/s for 90 nonlagged-like zones ( $\pm$ SD from 20 cells in layer 4). This compares with means of  $19 \pm 10$  and  $42 \pm 24$  spikes/s for lagged and nonlagged X-cells, respectively (Saul and Humphrey 1990b).

In summary, both separable and inseparable receptive fields were observed, as in previous studies. Measurements of response phase at a series of temporal frequencies permitted an association to be made between cortical responses and geniculate lagged and nonlagged responses. Cortical lagged-like responses could be reliably obtained from specific zones of certain receptive fields. Although at any one temporal frequency a lagged-type phase value could be explained in many ways, the correspondence of both latency and absolute phase between cortex and LGN limits the possibilities.

#### Population results

In the LGN, lagged and nonlagged cells could be distinguished by plotting their latencies versus their absolute phase values (Fig. 8 in Saul and Humphrey 1990b). In the present study, we measured these two response timing parameters at a series of positions across the receptive fields of 37 simple cells in area 17 from eight cats. These latency/absolute phase pairs are plotted in Fig. 14. As described above, points with large variability were rejected, so that all of these positions had standard deviations that were  $< 40$  ms in latency and  $< 0.1$  cycles in absolute phase (as well as satisfying the other conditions detailed above). The absolute phase values have been collapsed into a half-cycle, normalizing for the ON/OFF distinction. In Fig. 14A all 226 points are plotted, in Fig. 14B only the 134 points derived from 20 cells lying in or near layer 4 are shown, and in Fig. 14C data from the LGN are shown, separated by cell type (lagged or nonlagged and X or Y). Points with short latencies almost invariably fall in the nonlagged quarter-cycle (from  $-0.25$  to 0 cycles) of absolute phase. The longer latency points vary more in their absolute phase values, but predominate in the lagged quarter-cycle (0 to 0.25 cycles). As was true for the geniculate data, a latency of  $\sim 100$  ms appears to be a reasonable dividing line between points falling in these separate quarter-cycle regions. The area 17 and LGN distributions bear a striking resemblance, although points with

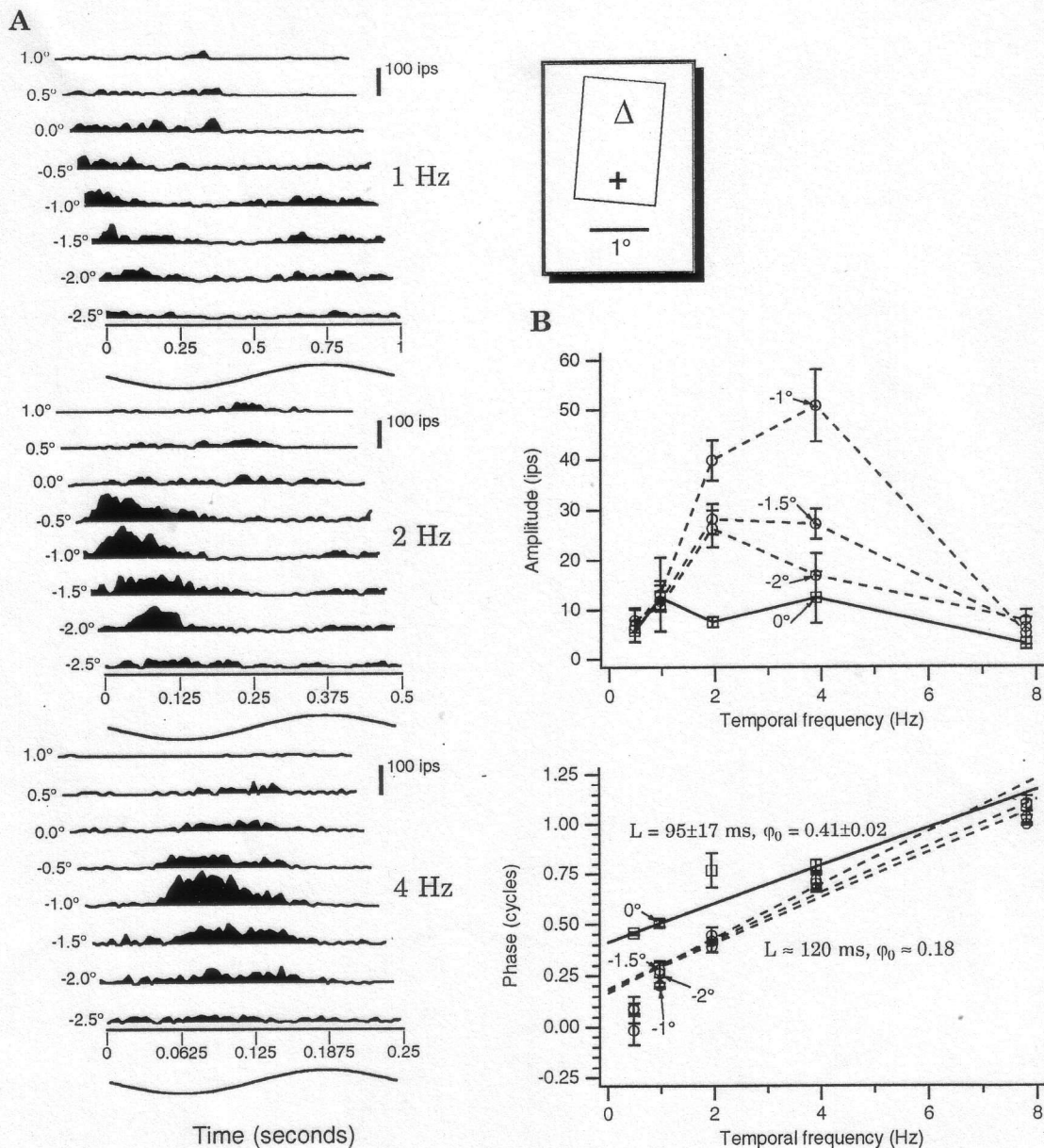


FIG. 12. Data from a cell with predominantly lagged-like responses. This cell was tested with a  $0.5 \times 6^\circ$  bar at 11 positions over  $5^\circ$  and at 5 temporal frequencies. *A*: histograms are shown for 8 of these positions and 3 temporal frequencies. These positions cover the receptive field, illustrated in the inset. Means and standard errors for amplitude and phase are shown for 4 of these positions in *B*. The dashed lines and open circles represent data from positions with lagged-like timing. Latencies of these 3 positions were 117, 133, and 113 ms, and their absolute phase values were 0.187, 0.166, and 0.181 cycles. The nonlagged-like responses at  $0^\circ$  are shown with solid lines and open squares. The intervening position,  $-0.5^\circ$ , had lagged-like latency and absolute phase values. At  $-2.5^\circ$  the absolute phase was 0.215, but the latency was 99 ms, just missing the cutoff to be classified as lagged-like. The cell's laminar location was undetermined.

long latencies and absolute phase leads are conspicuous in the cortical data. The percentage of points in each quadrant of these plots are given in Table 2. There are clearly cortical responses that are not directly accounted for by the geniculate data. Most of these anomalous points arise from cells outside of layer 4, suggesting their origin in intracortical processing or from inputs arising from outside the A-layers of the LGN (Malpeli et al. 1983, 1986). Results from cortical cells in layer 4, nearly all of which receive direct geniculate input (Bullier and Henry 1979b; Martin and Whitteridge 1984) look remarkably similar to those inputs (cf. Fig. 14, *B* and *C*).

We compared the latencies in cortex with those of X-cells in the LGN (X- and Y-cell latencies are almost identical within either the lagged or nonlagged groups). The average latency for the nonlagged-like positions (by definition these had latencies  $< 100$  ms) was  $78 \pm 13$  ms ( $n = 123$ ), with a range from 34 to 99 ms;  $X_N$ -cells had a mean of  $63 \pm 17$  ms ( $n = 77$ ), with a range from 37 to 107 ms. For the lagged-like positions, latencies averaged  $132 \pm 29$  ms ( $n = 52$ ), ranging up to 269 ms;  $X_L$ -cells averaged  $133 \pm 23$  ms ( $n = 33$ ) and ranged from 94 to 197 ms. Thus, nonlagged-like zones in cortex appear to have slightly longer latencies than nonlagged cells on average. There was no difference in la-

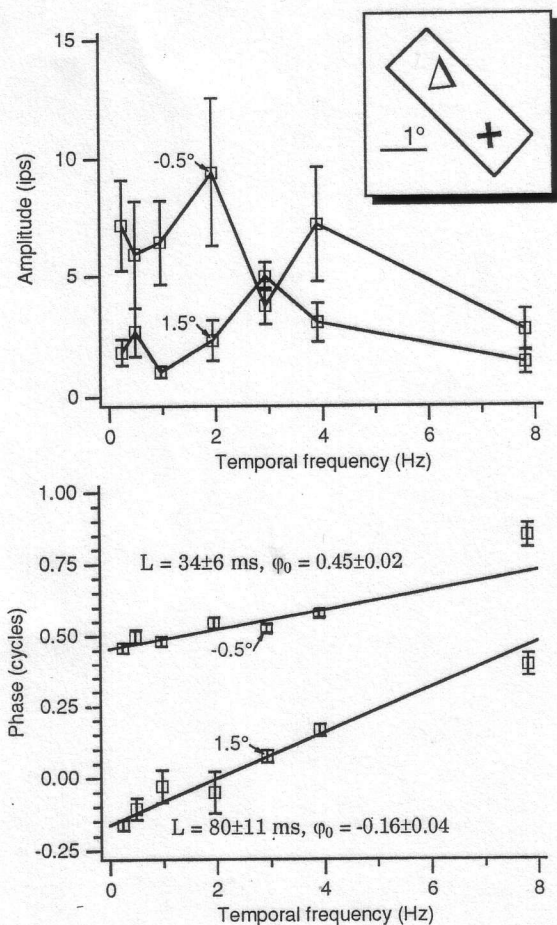


FIG. 13. Amplitude and phase values are plotted against temporal frequency for 2 positions from a layer 6 cell. These 2 positions were the most responsive in each subzone, despite testing at 21 positions with a  $0.5 \times 4^\circ$  bar. This illustrates that weak responses do not imply lagged-like timing, because all tested positions with adequate responses had nonlagged-like latency and absolute phase values in this cell.

tency statistics between the entire sample of cortical data and the subset of cells in layer 4. As can be seen in Fig. 14, absolute phase values were scattered across the full range in both cortex and LGN; the only difference between the geniculate and cortical data was a slightly higher average absolute phase value for cortical lagged-like positions ( $0.15 \pm 0.07$  cycles compared with  $0.08 \pm 0.09$  cycles for  $X_L$ -cells).

One of the main issues that should be addressed concerns the convergence of lagged and nonlagged afferents on single cells. Although the present methods are not particularly suited to answering such questions, the results can be suggestive. Lagged-like zones were generally accompanied by nonlagged-like zones, although in a few cells (e.g., Fig. 12) the lagged-like zones predominated. Each cell was classified as predominantly lagged, predominantly nonlagged, or mixed. These categories were not meant to indicate real cell classes (as opposed to S and C cells, e.g.), but only to help analyze further differences between cells that might correlate with response timing. Mixed cells had  $>20\%$  of their tested positions classified as lagged-like and  $>20\%$  nonlagged-like. Predominantly lagged or nonlagged cells had  $>20\%$  of their tested positions classified as lagged-like or nonlagged-like, respectively, and no more than 20% were the opposite type. With this admittedly arbitrary scheme, 8 cells were predominantly lagged, 21 cells were predomi-

nantly nonlagged, and 7 cells were mixed (Table 3). For one cell most of the positions tested could not be classified (i.e., the latency/absolute phase values fell in the second or fourth quadrant in Fig. 14). Of the 8 predominantly lagged cells, one had only 2 lagged-like positions out of 6, another had 4 lagged-like positions out of 8, and the other 6 such cells had from 60 to 100% lagged-like positions. These categories allow consideration of whether differences in latency, receptive-field dimensions, number of subzones, and laminar segregation correlate with the presence or absence of lagged-like and nonlagged-like zones.

Average latencies differ between these receptive-field categories, by definition. It is of interest, however, to consider the range of latencies observed within individual receptive fields (defined by the difference between maximum and minimum latencies, as shown in Table 3). Across the entire population, the average latency range in single cells was only 61 ms. If cortical cells sampled several lagged and nonlagged geniculate inputs randomly, and if the latencies of these inputs were reflected without change in the cortical receptive fields, this average range ought to be somewhat larger than the difference between the mean lagged and the mean nonlagged latencies,<sup>1</sup> which is 70 ms. Clearly, one or both of these hypotheses are invalid. The average range of latencies observed in the mixed cells was 89 ms, consistent with random sampling from the geniculate afferents. For predominantly lagged cells, the average latency range was 63 ms, and for the predominantly nonlagged cells the average range was 47 ms. The relatively restricted latency ranges of the predominantly nonlagged cells produced the compression seen in the combined population. The suggestion from this analysis is that cortical cells vary in the proportion of lagged and nonlagged inputs they receive, with many cells receiving minimal excitatory influences from lagged cells and others receiving their dominant geniculate drive from lagged cells. These differences in afferent connectivity should be correlated with other response properties, as well as having possible correlates in anatomic organization.

This categorization of cells was therefore compared with a measure of overall latency obtained from measuring phase versus temporal frequency in response to gratings drifting across the receptive field (Hamilton et al. 1989; Lee et al. 1981; Reid et al. 1992; Saul and Humphrey 1990b). A subset of 28 cells for which line-weighting function data were obtained were also tested with drifting gratings. Both directions were tested in these cells, although some cells did not respond adequately in their nonpreferred direction to permit reliable latency values to be derived. The predominantly lagged cells had slightly longer latencies in both directions compared with the predominantly nonlagged cells. Means and standard deviations were  $118 \pm 48$  ms for 7 predominantly lagged cells,  $93 \pm 18$  ms for 15 predominantly nonlagged cells, and  $107 \pm 45$  ms for 6 mixed cells tested in the preferred direction. For the nonpreferred direction, the corresponding values were  $106 \pm 50$  ( $n = 5$ ),  $78 \pm$

<sup>1</sup> The average range would be the mean of the difference between the maximum lagged latency and the minimum nonlagged latency, for samples of lagged and nonlagged inputs. For sample sizes  $>1$ , the expected value of the minimum of a sample is less than the mean of the sampled distribution, and similarly the expected value of the maximum of a sample is greater than the mean of the sampled distribution. Thus the average range would be greater than the difference between the means.

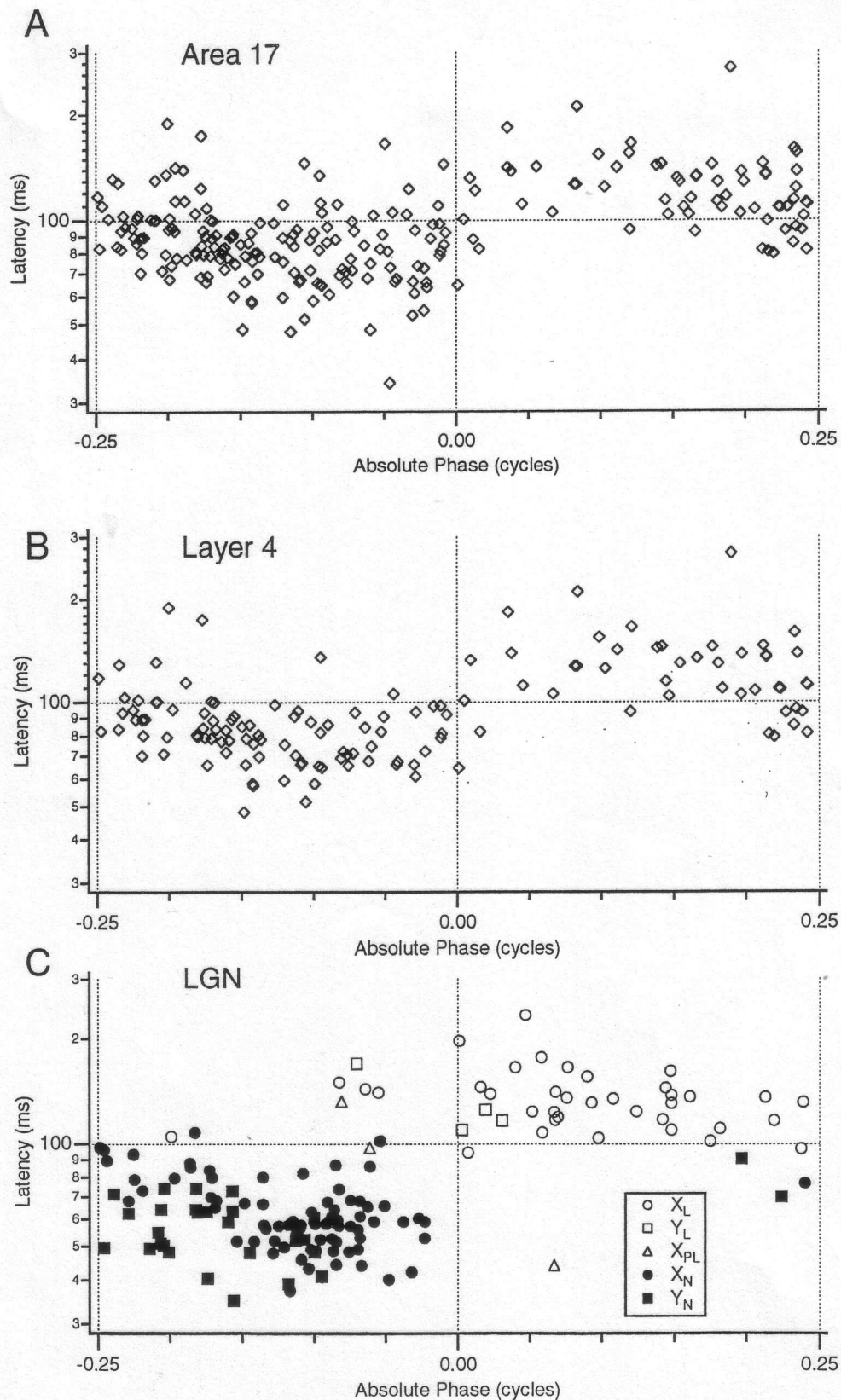


FIG. 14. *A*: population data summarizing the distributions of latency and absolute phase are shown for all 37 cells tested in area 17. *B*: the subset of 20 cells with somas located in or near layer 4. *C*: a sample of neurons from the A layers of the LGN. Cells were considered to be in or near layer 4 if they were clearly located in either layer 4 or lower layer 3, or if they were close enough (i.e., within subjective estimates of reconstruction errors) to the layer 4/5 border to be located in lower layer 4. Absolute phase values were collapsed into a half-cycle by subtracting 0.5 cycles when the original value exceeded 0.25 cycles. Sample sizes are 226 receptive field positions in *A*, 134 receptive field positions in *B*, and in *C*, 37  $X_L$  (lagged X) cells, 4  $Y_L$  (lagged Y) cells, 4  $X_{PL}$  (partially lagged X) cells, 80  $X_N$  (nonlagged X) cells, and 33  $Y_N$  (nonlagged Y) cells (replotted from Fig. 8 in Saul and Humphrey, 1990a, with 8 additional cells recorded in a more recent experiment with methods identical to those in the cortical experiments).

TABLE 2. Percentages of points in quadrants of latency/absolute phase space

	Lagged-Like		Nonlagged-Like	
	L > 100, $\varphi_0 > 0$	L > 100, $\varphi_0 < 0$	L < 100, $\varphi_0 < 0$	L < 100, $\varphi_0 > 0$
Area 17	24	17	53	6
Layer 4	26	10	57	8
LGN	22	5	70	4

L, latency;  $\varphi_0$ , absolute phase; LGN, lateral geniculate nucleus.

23 ( $n = 11$ ), and  $77 \pm 21$  ms ( $n = 6$ ). These independent measurements are therefore consistent with a hypothesis that the timing of the receptive-field zones, which may reflect that of the lagged and nonlagged afferents, influences global response properties.

A measure of the number of receptive-field subzones, based on the number of cycles of absolute phase observed across the receptive field, is given in Table 3. A cell with an ON and an OFF subzone would span  $\sim 0.5$  cycles, whereas a cell with three subzones would span  $\sim 1.0$  cycles. No trend was found for the number of subzones to vary with either receptive-field category or laminar position; Receptive-field dimensions did not seem to vary with these categories. Average receptive-field size was slightly smaller in the predominantly lagged cells ( $1.0 \times 0.9^\circ$ ) than in predominantly nonlagged cells ( $1.3 \times 1.1^\circ$ ) or mixed cells ( $1.6 \times 1.7^\circ$ ), but this could depend partly on the slightly lower average eccentricity of the predominantly lagged cells ( $3.8^\circ$  compared with  $5.4$  or  $5.3^\circ$ , respectively).

Estimates of laminar position were obtained for 32 of these 36 cells, judged without knowledge of the timing behavior of each cell (Table 3). Figure 15 presents the distribution of these categories across cortical layers. The predominantly lagged cells were found only in layer 4B (5

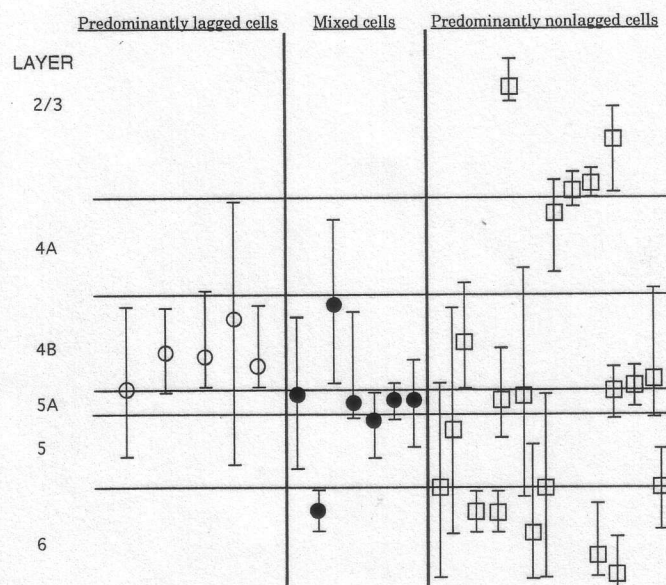


FIG. 15. Laminar locations of 32 cells are plotted for each of 3 categories based on response timing, as described in the text. Error bars indicate a subjective assessment of the maximum error in localizing recording sites. There is a clear tendency for cells showing lagged-like responses (predominantly lagged and mixed cells) to be found in layer 4B or 5A. Predominantly nonlagged cells were found in all layers.

TABLE 3. Individual cell results

Cell	Layer	No. of Cycles	$L_{\text{Min}}$ , ms	$L_{\text{Max}}$ , ms	No. of Zones	% Lag	% Nonlag
<i>Predominantly lagged cells</i>							
CX5 04	4B	1.0	93	154	7	86	14
CX6 07	4B	0.5	95	203	6	33	17
CX6 09	4B	1.0	112	145	5	100	0
CX7 02	U	0.6	124	155	3	67	0
CX7 04	U	0.6	101	142	5	60	0
CX8 11	4B	0.7	114	183	3	67	0
CX9 04	U	0.3	95	133	6	67	17
CX10 04	4B	0.8	86	211	8	50	12
<i>Mixed cells</i>							
CX5 05	5A	1.2	81	135	9	44	56
CX5 08	6	0.8	82	142	7	43	29
CX6 03	4B	0.1	92	132	3	33	67
CX9 02	5A	1.0	52	114	13	31	62
CX10 10	5	0.3	77	145	3	33	33
CX10 11	5A	1.0	69	269	6	50	33
CX11 15	5A	0.8	66	210	7	29	57
<i>Predominantly nonlagged cells</i>							
CX4 08	5/6	0.5	66	104	4	0	50
CX4 09	5	1.0	61	111	4	0	50
CX5 03	4B	0.7	61	86	4	0	75
CX5 09	6	1.5	84	136	8	12	50
CX5 11	6	0.7	53	114	6	17	67
CX6 04	5A	0.5	67	97	5	0	100
CX6 11	3	0.9	85	111	4	0	25
CX7 01	U	0.6	67	95	5	0	100
CX8 03	5A	0.9	66	189	9	11	67
CX8 04	6	0.7	55	146	6	17	67
CX8 05	5/6	0.3	64	142	8	0	62
CX8 17	4A	0.5	65	76	7	0	100
CX8 18	3/4	1.0	79	105	9	0	67
CX8 19	3/4	1.1	66	117	5	0	60
CX9 05	6	0.4	88	132	5	20	60
CX9 07	6	0.6	34	80	5	0	100
CX10 02	3	0.5	87	166	5	0	80
CX10 13	4B	1.1	67	139	13	8	85
CX10 14	4B	0.9	48	86	7	0	86
CX11 07	4B	0.5	79	101	5	20	60
CX11 14	5/6	1.0	74	112	8	0	50
<i>Unclassified cell</i>							
CX8 16	4A	0.6	81	104	6	17	17

The no. of cycles refers to the difference between minimum and maximum absolute phase values observed across receptive field. The no. of zones refers to the number of positions that provided admissible latency and absolute phase values.  $L_{\text{Min}}$  and  $L_{\text{Max}}$ , minimum or maximum latency observed in receptive field; %Lag and %Nonlag, percentage of admissible positions that were lagged-like or nonlagged-like; U, unknown layer.

cells). The mixed cells were found mainly in layers 4B or 5A (5 cells); one was found in 5B and another in layer 6. The predominantly nonlagged cells were distributed fairly evenly across cortex, with 10 of the 20 reconstructed found in or near layer 4. All four of the cells located in layer 4A or lower layer 3 were predominantly nonlagged. This sample provides evidence that lagged-like responses can be observed in lower layer 4 and the 4/5 border region.

## DISCUSSION

### Summary and major interpretations

Our main finding is that evidence of lagged and nonlagged geniculate inputs can be detected in the receptive

fields of simple cells in cortical area 17. We used the distinction between these inputs based on response timing. Because we expected that the lagged and nonlagged pathways might converge in cortex, it was necessary to look for spatially segregated inputs to single cells, which was accomplished by obtaining line-weighting functions with sinusoidal luminance-modulation. Analysis of the line-weighting data revealed the existence of responses having timing similar to that of geniculate cells. Some simple cells display classical ON and OFF zones, in which response timing between zones differs by a half-cycle. In other cells there are receptive-field zones with response timing intermediate between classical ON and OFF zones, as seen in previous studies (Dean and Tolhurst 1986; McLean and Palmer 1989; Movshon et al. 1978; Reid et al. 1987, 1988, 1991; Tolhurst and Dean 1991). We have shown that response phase increases more rapidly with temporal frequency in these zones than in the classical ON and OFF zones. For some cortical cells, at certain receptive-field positions, the responses resemble those of lagged geniculate cells, with absolute phase lags and long (>100 ms) latencies. Many cells also show nonlagged-type responses, with absolute phase leads and short (<100 ms) latencies. These lagged-like and nonlagged-like responses remained consistent across repeated tests. The distribution of latency and absolute phase values from cells in the geniculocortical recipient zone resemble closely the distribution of these two key parameters in the LGN.

A striking finding was that most lagged-like responses were seen in layer 4B and immediately below in layer 5A. This is consistent with independent evidence that lagged cells terminate predominantly in lower layer 4. Current-source density measurements derived from electrical stimulation of the LGN revealed long-latency (2–10 ms) sinks in lower layer 4, compared with shorter-latency (1.5–2.5 ms) sinks in upper layer 4 (Mitzdorf and Singer 1978). These two latency ranges match the respective ranges of antidromic latencies for lagged and nonlagged cells (Humphrey and Weller 1988a; Mastronarde 1987a). Also, cells in layer 4B tend to be difficult to drive by electrical stimulation of the retinogeniculostriate pathway (Martin and Whitteridge 1984), paralleling the difficulty of activating lagged LGN cells by optic chiasm stimulation (Humphrey and Weller 1988a; Mastronarde 1987a). Soma size distributions obtained by injections of retrograde label in cortical sublaminae indicate that a population of small A-layer cells projects to layer 4B but not to layer 4A (Leventhal 1979). These cells are similar in soma size to lagged X-cells (Humphrey and Weller 1988b). The existence of layer 5A cells with lagged-like response signatures is not incompatible with a concentration of lagged afferents in layer 4B. Many layer 5A pyramidal neurons have basal dendrites that arborize in layer 4B, allowing them to sample the geniculate input directly (Lund et al. 1979; Martin and Whitteridge 1984). We also observed nonlagged-like responses in layer 4B, consistent with data showing that nonlagged X-axons project to both layers 4A and 4B (Freund et al. 1985; Humphrey et al. 1985).

In the following sections, we consider a number of issues raised by these results and interpretations. First, the impact of our methods on these findings is discussed. Next, we argue that lagged-like and nonlagged-like responses arise from lagged and nonlagged inputs, respectively, and that it

is unlikely that the lagged-like responses are generated from purely nonlagged inputs. Finally, we briefly mention a possible functional role for these inputs.

#### *Methodological issues*

The present study employed the methods of our previous investigation of the LGN, with two notable exceptions. We tested LGN cells primarily with small spots centered in the receptive fields. For cortical cells, we used long bars of optimal orientation. This difference is relatively unimportant to the present results, because we have also tested many geniculate cells with bars in addition to spots and have found no difference in response timing for these two stimuli, consistent with other LGN results which showed that the lagged/nonlagged distinction is not affected by spot size (Humphrey and Weller 1988a; Mastronarde 1987a). In fact, measuring response profiles to bars drifting across geniculate cell receptive fields in each direction is an excellent way to distinguish these two cell types (Mastronarde 1987a; Saul and Humphrey 1990a). For cortical cells, the problem arises that one is presumably stimulating many afferents, especially when using long bars. This should bias the cortical results away from seeing response timing like that in the LGN, so to the extent that lagged- and nonlagged-like timings were observed it appears that the use of bars was not critical. Another difference between this study and the previous LGN work is the use of barbiturate anesthesia for the LGN recordings. In other experiments in this lab and elsewhere (Heggelund and Hartveit 1990; Humphrey and Saul 1992), samples of LGN cells have been obtained under halothane anesthesia like that used here, with results identical to those seen under barbiturate anesthesia.

Our concentration on simple cells does not imply that lagged input might be targeted exclusively to these neurons rather than to complex cells as well. The methods used here are directly applicable only to simple cells, and this restricted our sampling. Complex cells do not respond well in general at the fundamental frequency of a visual stimulus, and our measures of response timing in the LGN are based on such responses. More elaborate methods and arguments are needed to test for the presence of lagged input to complex cells.

Response amplitudes in lagged-like zones were sometimes weaker than in nonlagged-like zones. Regardless of whether these two types of response timing are inherited from the LGN, or are generated by intracortical mechanisms, lagged-like zones did not appear to be artifacts arising from poor response quality. Occasional lagged-like responses were observed that were at least as vigorous as the nonlagged-like responses from neighboring positions or from other cells, and on average lagged-like zones had peak response amplitudes almost as high as nonlagged-like zones. Only responses that satisfied objective criteria for reliability were admitted to guard against interpreting weak and/or variable responses as lagged-like.

Our use of linear regression to estimate parameters that serve to identify lagged-like and nonlagged-like responses can be questioned because phase versus temporal frequency data often show a slight convexity that is neglected by the linear fit. However, the same convexity is present in the LGN data (Saul and Humphrey 1990b). This deviation

from linearity occurs at the lowest and highest temporal frequencies, where response amplitudes are weakest and phase variability is high. The lines fit the data best between 1 and 4 Hz, generally the range of temporal frequencies where cells respond best. Our fitting procedure accurately estimates the latency that would be produced by delays and low-pass filtering (Reid et al. 1992). Cortical latencies are not substantially greater than LGN latencies (Hamilton et al. 1989; Lee et al. 1981; Reid et al. 1992). Why do conduction delays and additional temporal filtering not increase latencies between the LGN and visual cortex? The additional geniculocortical conduction latency of 1–2 ms for nonlagged and 2–10 ms for lagged cells (Mastrorarde 1987a; Humphrey and Weller 1988a) is too small to be noticed in the present data, where mean latencies ranged from 34 to 270 ms, and standard deviations were generally  $>2$  ms. Similarly, the cortical latency cutoff point between lagged-like and nonlagged-like zones should be  $>100$  ms, given the longer geniculocortical latencies for lagged cells. Again, this difference amounts to only a few milliseconds on average and would not necessarily show up in the scatter of cortical latencies. This leaves the question of why cortical low-pass filtering does not seem to contribute additional integration time. Cortical filtering may include high-pass as well as low-pass mechanisms, and these high-pass filters could reduce the integration time. The data suggest that low-pass filtering is not as prominent a feature of cortex as might be presumed from the apparent loss of temporal resolution between LGN and cortex (Orban et al. 1985; Saul and Humphrey 1992). We suspect that low-pass filters, which produce outputs with phase lags relative to their inputs, could not produce the absolute phase lag associated with lagged-type responses, because such filters create a phase lag predominantly at higher frequencies. However, our use of linear regression to analyze the phase versus temporal frequency data does not allow this possibility to be excluded. The absolute phase values derived by these methods for LGN cells provided the key to understanding their response profiles to luminance step stimuli, distinguishing not only lagged and nonlagged cells but also tonic and phasic cells (Saul and Humphrey 1990b). This indicates that the latency and absolute phase parameters capture the cell's behavior in response to most stimuli, besides providing measures of timing that are convenient. The slope and intercept of the regression lines seem to reflect important characteristics with implications for mechanisms (Hamilton et al. 1989; Reid et al. 1992; Saul and Humphrey 1990b), but here they are used mainly as a tool to identify cortical response types.

#### *Interpreting cortical responses as arising from geniculate inputs*

We consider here alternatives to the proposition that cortical lagged-like responses arise from lagged inputs.

Could all of the response timing behaviors observed here be explained in terms of differences within the population of nonlagged inputs? The sustained/transient dichotomy (which is distinct from, although somewhat correlated with, the X/Y classification) provides a potential means to explain some of the temporal behavior we observed, because completely sustained responses and completely tran-

sient responses differ by a quarter-cycle of response phase (Saul and Humphrey 1990b). For instance, a transient ON-center nonlagged LGN cell has an absolute phase value near  $-0.25$  cycles, and a sustained ON-center cell has absolute phase near  $0.0$  cycles. Timing differences between sub-zones in cortical cells can thus be generated by convergence of nonlagged afferents having varying degrees of tonicity. Could the lagged-like responses we see be explained in terms of such inputs? At any single temporal frequency, it can be difficult to distinguish lagged and nonlagged responses. For instance, at 1 Hz, sustained ON-center nonlagged and lagged cells both have response phase values  $\sim 0.05$  cycles; transient ON-center lagged cells and transient OFF-center nonlagged cells both have response phase  $\sim 0.35$  cycles (Saul and Humphrey 1990b). However, lagged and nonlagged responses are easily distinguished when followed across temporal frequency, as was done here. The key distinguishing features are the longer latencies and absolute phase lags associated with lagged responses. Cortical lagged-like responses have different absolute phase and latency values than either transient or sustained nonlagged inputs; their phase behavior instead indicates that they arise from lagged inputs. It should be noted, nonetheless, that within either the lagged or nonlagged geniculate populations there exists a full and continuous range of response timing, and this range may contribute to the range of cortical response timing (Fig. 14).

Could these lagged-like response timings arise from simultaneous activation of nonlagged ON and OFF zones? This seems unlikely but is admittedly possible and unsettled by the present experiments. Responses of opposite polarity do not add up to one of the intermediate values but instead cancel each other. On the other hand, vector addition of ON and OFF responses that are more than a third of a cycle apart would lead to reduced response amplitudes, perhaps like those observed in the lagged-like zones. One could argue that, for example, a transient ON-response and a sustained OFF-response could combine to look like a lagged OFF-response. Such an arrangement may occur in cells, but does not produce a lagged-like dependence on temporal frequency. Lagged-like latencies would arise from combining nonlagged inputs only under special circumstances. For instance, the transient input must be tuned to higher temporal frequencies than the sustained input, or low-pass filtering must occur. Adding two nonlagged-like responses to obtain absolute phase lags should produce responses with short latencies as often as long latencies. The fact that short latencies are rarely associated with absolute phase lags presents a strong argument against this hypothesis. Moreover, if convergence of nonlagged inputs were responsible for the lagged-like responses observed, one would expect bar width to influence occurrence of lagged-type responses. A dependence of timing on bar width was not observed.

Combinations of excitatory and inhibitory nonlagged-like inputs could certainly produce lagged-like responses, especially in combination with other intracortical and cellular mechanisms. Because a lagged output is generated in the LGN from a nonlagged retinal input (Mastrorarde 1987b), cortical regeneration of such responses is possible. The only argument against this for now relies on the existence of lagged inputs to visual cortex, which comprise  $\sim 40\%$  of the X-afferents there, and our finding that the

laminar distribution of nearly all lagged-like responses matches the apparent laminar terminations of lagged afferents.

Although we have detected the influence of lagged afferents in cortex, we cannot distinguish whether they arose from  $X_L$ -cells or  $Y_L$ -cells.  $Y_L$ -cells tend to have smaller absolute phase lags than  $X_L$ -cells, but overlap on this measure precludes clear identification even in the LGN (Fig. 14). Nevertheless, we suspect that  $X_L$ -cells contributed most to our recordings because they are more plentiful in the LGN, comprising 40% of X-afferents, than  $Y_L$ -cells, which may comprise only 5% of the Y-afferents arising from the A-laminae (Humphrey and Weller 1988a; Mastronarde 1987a; Mastronarde et al. 1991). Note that our inability to distinguish X and Y types is unimportant in this study; response timing in  $X_L$ - and  $Y_L$ -cells is similar and readily distinguishable from the timing of  $X_N$ - and  $Y_N$ -cells (Saul and Humphrey 1990b). The possibility that some of the lagged-like response timing reflects the influence of W-cells can not be completely discounted, because the C-laminae (where W-cells are found) project to lower layer 4 and upper layer 5 (LeVay and Gilbert 1976; Leventhal 1979). However, this projection also includes upper layer 4 and lower layer 3, where we did not observe lagged-like responses. The large receptive fields of most W-cells (Cleland et al. 1975; Sur and Sherman 1982; Wilson et al. 1976) argues against their role in forming the small subzones of cortical receptive fields considered here.

An important question is whether the lagged-like cortical responses arose directly from the afferents via monosynaptic activation or indirectly from them via activation of other cortical cells. Although our data do not expressly address this, it is possible that direct inputs contribute significantly to the responses because virtually all cells in layer 4 and many cells in layer 5A are monosynaptically activated from the LGN (Bullier and Henry 1979b; Ferster and Lindstrom 1983; Martin and Whitteridge 1984), and these afferents can make a significant contribution to the responses of cortical cells (Tanaka 1983a). Similarly, direct geniculate inputs may underlie the nonlagged-like cortical responses in these layers. However, even in layer 4 the majority of inputs to cortical cells arise from other cortical cells (Davis and Sterling 1979), and it is unclear what roles afferent versus intracortical connections play in shaping the spatiotemporal structure of the cortical receptive field. Nevertheless, our working hypothesis, based on the laminar analysis, is that the lagged-like responses primarily reflect direct geniculate drive.

We found that the degree to which cortical cells were influenced by lagged and nonlagged inputs varied. A few cortical cells were classified as mixed cells, on the basis of their displaying lagged-like and nonlagged-like timing at separate points in the receptive field. This implies that these two afferent streams converge on some simple cells. Many other cells had few or no lagged-like zones, and several cells had few or no nonlagged-like zones. This suggests that in these latter cells the lagged and nonlagged pathways remain separate. However, our methods do not exhaustively test the inputs to cells. Only relatively strong, spatially segregated, excitatory inputs are revealed. Thus we can not be sure that neurons did not have additional inputs to those inferred. Our results represent a lower bound on the affer-

ent connectivity, primarily providing evidence for the existence of lagged and nonlagged inputs.

Simple cell receptive fields appear to be constructed in part by excitatory convergence of several geniculate inputs. These inputs may be ON- or OFF-center, lagged or nonlagged, and phasic or tonic. The receptive fields of these inputs probably overlap somewhat but are sufficiently segregated to permit response timing to vary across space (whereas in complex cells this is not the case). The progression of response timing across inseparable receptive fields such as the one illustrated in Fig. 6 may reflect a progression through offset lagged and nonlagged receptive fields. To what extent the responses obtained at any given position reflect activation of single afferents as opposed to a weighted average of several inputs remains untested. We suspect that in the present experiments each narrow bar probably stimulated several afferents, but the dominant afferent type varied across the receptive field. In many cells the arrangement of afferents appears to be organized such that lagged and nonlagged inputs interdigitate, with a monotonic progression of response phase across space. Such an arrangement produces spatiotemporally inseparable receptive fields and direction selectivity. In some cells the afferents presumably are not organized in such a rigid manner, and these cells are less direction selective, and response phase is not monotonic across space.

The similarity between response timing in cortical receptive fields and in geniculate afferents argues for the construction of cortical fields from excitatory convergence of these afferents. But whereas lagged and nonlagged cells can be easily recorded throughout the A-laminae of the LGN, lagged-like responses tended to be more difficult to find in many cortical cells. Cortical receptive fields are not constructed simply by passive acceptance of convergent afferent inputs, however. Direct excitation from the geniculate plays a key role in building receptive fields, but intracortical interactions probably modify this framework extensively. In particular, inhibitory intracortical inputs undoubtedly sculpt the receptive field profile. In addition, active processes probably contribute to cortical response timing, just as they appear to create lagged responses in the LGN. The differences observed between the geniculate and cortical results may be attributable to these cortical processing mechanisms.

One might expect intracortical mechanisms to become increasingly apparent, moving from the geniculate recipient layers to the superficial layers and layer 5. Therefore, it should become more difficult to detect lagged-like and nonlagged-like responses as the ordinal position of cells increases. Our results suggest that excitatory lagged-type responses are observed primarily in layer 4B and immediately below in layer 5A. The effects of lagged-like cortical responses on neurons in other layers could be important but would not necessarily reflect the geniculate signature of long latencies and absolute phase lags, particularly if they arose from inhibitory local circuit neurons. Many cells outside layers 4 and 6 are also dependent on inputs from the C-laminae and MIN, either from direct geniculocortical projections to area 17 or from projections to area 18 whose cells then project back to area 17 (Bullier and Henry 1979a; Malpeli et al. 1986). These various inputs have not been characterized the way the A layer cells have been, giving

even more reason not to expect cortical cells in upper layers to behave like lagged and nonlagged cells.

### Functional implications

The data presented here provide evidence that lagged and nonlagged afferents converge onto single simple cells and contribute to the spatiotemporal structure of the receptive field by setting up timing differences between spatially separated regions. Gradients in response timing across receptive fields are correlated with direction selectivity (Hamilton et al. 1989; McLean and Palmer 1989; Reid et al. 1987, 1991; Saul and Humphrey 1990a; Tolhurst and Dean 1991). The potential importance of lagged and nonlagged inputs for this functional role lies in their timing difference at low temporal frequencies. Simple cells often have responses in one zone that lag the stimulus and responses in another zone that lead the stimulus at low frequencies. The firing in these two zones occurs hundreds of milliseconds apart; achieving these long delays by intracortical mechanisms would require extraordinary neuronal processing. The lagged and nonlagged afferents may provide these timing differences, not as delays, but as approximately quarter-cycle phase differences that are maintained from very low temporal frequencies up to  $\sim 4$  Hz (Saul and Humphrey 1990b). Above 4 Hz the timing differences between the afferents increases to about a half-cycle. In cortex, the timing differences between subzones in simple cells often follow this pattern of quarter-cycle phase differences at low temporal frequencies which increase to about a half-cycle by 4 Hz (cf. Figs. 8, 11, and 12). This temporal frequency dependent phase behavior in cortex has a parallel in a temporal frequency dependent direction selectivity. Many cortical cells are direction selective at low temporal frequencies but lose their direction selectivity at  $\sim 4$  Hz (Saul and Humphrey 1992). These relationships suggest that the timing differences between lagged and nonlagged cells, which are generated in the LGN, may contribute to the creation of direction selectivity in cortex. We are presently investigating this possibility.

We thank C. Lucci and P. Baker for computer programming.

This research was supported by National Institutes of Health Grants EY-06459 to A. L. Humphrey, MH-18273, and BNS-9021495 to A. B. Saul, and a Core Grant for Vision Research (EY-08098) to the Eye and Ear Institute of Pittsburgh.

Address reprint requests to A. B. Saul.

Received 20 March 1992; accepted in final form 28 May 1992.

### REFERENCES

- ADELSON, E. H. AND BERGEN, J. R. Spatiotemporal energy models for the perception of motion. *J. Opt. Soc. Am.* 2: 284-299, 1985.
- ALBRECHT, D. G. AND GEISLER, W. S. Motion selectivity and the contrast-response function of simple cells in the visual cortex. *Visual Neurosci.* 7: 531-546, 1991.
- BULLIER, J. AND HENRY, G. H. Neural path taken by afferent streams in striate cortex of the cat. *J. Neurophysiol.* 42: 1264-1270, 1979a.
- BULLIER, J. AND HENRY, G. H. Laminar distribution of first-order neurons and afferent terminals in cat striate cortex. *J. Neurophysiol.* 42: 1271-1281, 1979b.
- BULLIER, J., MUSTARI, M. J., AND HENRY, G. H. Receptive-field transformations between LGN neurons and S-cells of cat striate cortex. *J. Neurophysiol.* 47: 417-438, 1982.
- CITRON, M. C., EMERSON, R. C., AND IDE, L. S. Spatial and temporal receptive-field analysis of the cat's geniculocortical pathway. *Vision Res.* 21: 385-396, 1981.
- CLELAND, B. G., MORSTYN, R., WAGNER, H. G., AND LEVICK, W. R. Long-latency retinal input to lateral geniculate neurones of the cat. *Brain Res.* 91: 306-310, 1975.
- DAVIS, T. L. AND STERLING, P. Microcircuitry of cat visual cortex: classification of neurons in layer IV of area 17, and identification of the patterns of lateral geniculate input. *J. Comp. Neurol.* 188: 599-628, 1979.
- DE VALOIS, R. L., ALBRECHT, D. G., AND THORELL, L. G. Spatial frequency selectivity of cells in macaque visual cortex. *Vision Res.* 22: 545-559, 1982.
- DEAN, A. F. AND TOLHURST, D. J. Factors influencing the temporal phase of response to bar and grating stimuli for simple cells in the cat striate cortex. *Exp. Brain Res.* 62: 143-151, 1986.
- DERRINGTON, A. M. AND FUCHS, A. F. Spatial and temporal properties of X and Y cells in the cat lateral geniculate nucleus. *J. Physiol. Lond.* 293: 347-364, 1979.
- FERSTER, D. X- and Y-mediated synaptic potentials in neurons of areas 17 and 18 of cat visual cortex. *Visual Neurosci.* 4: 115-133, 1990.
- FERSTER, D. AND JAGADEESH, B. Nonlinearity of spatial summation in simple cells of areas 17 and 18 of cat visual cortex. *J. Neurophysiol.* 66: 1667-1679, 1991.
- FERSTER, D. AND LEVAY, S. The axonal arborizations of lateral geniculate neurons in the striate cortex of the cat. *J. Comp. Neurol.* 182: 923-944, 1978.
- FERSTER, D. AND LINDSTRÖM, S. An intracellular analysis of geniculocortical connectivity in area 17 of the cat. *J. Physiol. Lond.* 342: 181-215, 1983.
- FREUND, T. F., MARTIN, K. A. C., AND WHITTERIDGE, D. Innervation of cat visual areas 17 and 18 by physiologically identified X- and Y-type thalamic afferents. I. Arborization patterns and quantitative distribution of postsynaptic elements. *J. Comp. Neurol.* 242: 263-274, 1985.
- GAREY, L. J. AND POWELL, T. P. S. An experimental study of the termination of the lateral geniculo-cortical pathway in the cat and monkey. *Proc. R. Soc. Lond. B. Biol. Sci.* 179: 41-63, 1971.
- HAMILTON, D. B., ALBRECHT, D. G., AND GEISLER, W. S. Visual cortical receptive fields in monkey and cat: spatial and temporal phase-transfer function. *Vision Res.* 29: 1285-1308, 1989.
- HEGGELUND, P. AND HARTVEIT, E. Neurotransmitter receptors mediating excitatory input to cells in the cat lateral geniculate nucleus. I. Lagged cells. *J. Neurophysiol.* 63: 1347-1360, 1990.
- HOFFMAN, K.-P. AND STONE, J. Conduction velocity of afferents to cat visual cortex: a correlation with cortical receptive field properties. *Brain Res.* 32: 640-646, 1971.
- HUBEL, D. H. AND WIESEL, T. N. Receptive fields of single neurones in the cat's visual cortex. *J. Physiol. Lond.* 148: 574-591, 1959.
- HUBEL, D. H. AND WIESEL, T. N. Integrative action in the cat's lateral geniculate body. *J. Physiol. Lond.* 155: 385-198, 1961.
- HUBEL, D. H. AND WIESEL, T. N. Receptive fields, binocular interaction, and functional architecture in the cat's visual cortex. *J. Physiol. Lond.* 160: 106-154, 1962.
- HUMPHREY, A. L. AND SAUL, A. B. Action of brain stem reticular afferents on lagged and nonlagged cells in the cat lateral geniculate nucleus. *J. Neurophysiol.* 68: 000-000, 1992.
- HUMPHREY, A. L., SUR, M., UHLRICH, D. J., AND SHERMAN, S. M. Projection patterns of individual X- and Y-cell axons from the lateral geniculate nucleus to cortical area 17 in the cat. *J. Comp. Neurol.* 233: 159-189, 1985.
- HUMPHREY, A. L. AND WELLER, R. E. Functionally distinct groups of X-cells in the lateral geniculate nucleus of the cat. *J. Comp. Neurol.* 268: 429-447, 1988a.
- HUMPHREY, A. L. AND WELLER, R. E. Structural correlates of functionally distinct X-cells in the lateral geniculate nucleus of the cat. *J. Comp. Neurol.* 268: 448-468, 1988b.
- LEE, B. B., CLELAND, B. G., AND CREUTZFELDT, O. D. The retinal input to cells in area 17 of the cat's cortex. *Exp. Brain Res.* 30: 527-538, 1977.
- LEE, B. B., ELEPFANDT, A., AND VIRSU, V. Phase of responses to sinusoidal gratings of simple cells in cat striate cortex. *J. Neurophysiol.* 45: 818-828, 1981.
- LEHKUHL, S., KRATZ, K. E., MANGEL, S. C., AND SHERMAN, S. M. Spatial and temporal sensitivity of X- and Y-cells in dorsal lateral geniculate nucleus of the cat. *J. Neurophysiol.* 43: 520-541, 1980.
- LEVAY, S. AND GILBERT, C. D. Laminar patterns of geniculocortical projections in the cat. *Brain Res.* 113: 1-19, 1976.

- LEVENTHAL, A. G. Evidence that the different classes of relay cells of the cat's lateral geniculate nucleus terminate in different layers of the striate cortex. *Exp. Brain Res.* 37: 349-372, 1979.
- LUND, J. S., HENRY, G. H., MACQUEEN, C. L., AND HARVEY, A. R. Anatomical organization of the primary visual cortex (area 17) of the cat: a comparison with area 17 of the macaque monkey. *J. Comp. Neurol.* 184: 599-618, 1979.
- MALPELI, J. G. Activity of cells in area 17 of the cat in absence of input from layer A of lateral geniculate nucleus. *J. Neurophysiol.* 49: 595-610, 1983.
- MALPELI, J. G., LEE, C., SCHWARK, H. D., AND WEYAND, T. G. Cat area 17. I. Pattern of thalamic control of cortical layers. *J. Neurophysiol.* 56: 1062-1073, 1986.
- MARTIN, K. A. C. AND WHITTERIDGE, D. Form, function and intracortical projections of spiny neurones in the striate visual cortex of the cat. *J. Physiol. Lond.* 353: 463-504, 1984.
- MASTRONARDE, D. N. Two classes of single-input X-cells in cat lateral geniculate nucleus. I. Receptive-field properties and classification of cells. *J. Neurophysiol.* 57: 357-380, 1987a.
- MASTRONARDE, D. N. Two classes of single-input X-cells in cat lateral geniculate nucleus. II. Retinal inputs and the generation of receptive-field properties. *J. Neurophysiol.* 57: 381-413, 1987b.
- MASTRONARDE, D. N., HUMPHREY, A. L., AND SAUL, A. B. Lagged Y-cells in the cat lateral geniculate nucleus. *Visual Neurosci.* 7: 191-200, 1991.
- MCLEAN, J. AND PALMER, L. A. Contribution of linear spatiotemporal field structure to velocity selectivity of simple cells in area 17 of cat. *Vision. Res.* 29: 675-679, 1989.
- MITZDORF, U. AND SINGER, W. Prominent excitatory pathways in the cat visual cortex (A 17 and A 18): a current source density analysis of electrically evoked potentials. *Exp. Brain Res.* 33: 371-394, 1978.
- MOVSHON, J. A., THOMPSON, I. D., AND TOLHURST, D. J. Spatial summation in the receptive fields of simple cells in the cat's striate cortex. *J. Physiol. Lond.* 283: 53-77, 1978.
- MULLIKIN, W. H., JONES, J. P., AND PALMER, L. A. Receptive-field properties and laminar distribution of X-like and Y-like simple cells in cat area 17. *J. Neurophysiol.* 52: 350-371, 1984.
- ORBAN, G. A., HOFFMANN, K.-P., AND DUYSSENS, J. Velocity selectivity in the cat visual system. I. Responses of LGN cells to moving bar stimuli: a comparison with cortical areas 17 and 18. *J. Neurophysiol.* 54: 1026-1049, 1985.
- REID, R. C. *Directional Selectivity and the Spatiotemporal Structure of the Receptive Fields of Simple Cells in Cat Striate Cortex* (PhD thesis). New York: The Rockefeller Univ., 1988.
- REID, R. C., SOODAK, R. E., AND SHAPLEY, R. M. Linear mechanisms of directional selectivity in simple cells of cat striate cortex. *Proc. Natl. Acad. Sci. USA* 84: 8740-8744, 1987.
- REID, R. C., SOODAK, R. E., AND SHAPLEY, R. M. Directional selectivity and spatiotemporal structure of receptive fields of simple cells in cat striate cortex. *J. Neurophysiol.* 66: 505-529, 1991.
- REID, R. C., VICTOR, J. D., AND SHAPLEY, R. M. Broad-band temporal stimuli decrease the integration time of neurons in cat striate cortex. *Visual Neurosci.* In press.
- SAUL, A. B. AND HUMPHREY, A. L. Evidence of lagged-type geniculate input to visual cortex. *Soc. Neurosci. Abstr.* 16: 1218, 1990a.
- SAUL, A. B. AND HUMPHREY, A. L. Spatial and temporal response properties of lagged and nonlagged cells in cat lateral geniculate nucleus. *J. Neurophysiol.* 64: 206-224, 1990b.
- SAUL, A. B. AND HUMPHREY, A. L. Cortical direction selectivity as a function of temporal frequency. *Soc. Neurosci. Abstr.* 17: 1015, 1991.
- SAUL, A. B. AND HUMPHREY, A. L. Temporal frequency tuning of direction selectivity in cat visual cortex. *Visual Neurosci.* 8: 365-372, 1992.
- SCHILLER, P. H. Central connections of the retinal ON and OFF pathways. *Nature Lond.* 297: 580-583, 1982.
- SESTOKAS, A. K. AND LEHMKUHL, S. Visual response latency of X- and Y-cells in the dorsal lateral geniculate nucleus of the cat. *Vision Res.* 26: 1041-1054, 1986.
- SHERK, H. AND HORTON, J. C. Receptive field properties in the cat's area 17 in the absence of on-center geniculate input. *J. Neurosci.* 4: 381-393, 1984.
- SHERMAN, S. M. Functional organization of the W-, X-, and Y-cell pathways: a review and hypothesis. In: *Progress in Psychobiology and Physiological Psychology*, edited by J. M. Sprague and A. N. Epstein. New York: Academic, 1985, vol. 11, p. 233-314.
- SINGER, W., TRETTER, F., AND CYNADER, M. Organization of cat striate cortex: a correlation of receptive field properties with afferent and efferent connections. *J. Neurophysiol.* 38: 1080-1098, 1975.
- STONE, J. AND DREHER, B. Projection of X- and Y-cells of the cat's lateral geniculate nucleus to areas 17 and 18 of visual cortex. *J. Neurophysiol.* 36: 551-567, 1973.
- STONE, J., DREHER, B., AND LEVENTHAL, A. Hierarchical and parallel mechanisms in the organization of visual cortex. *Brain Res. Rev.* 1: 345-394, 1979.
- SUR, M. AND SHERMAN, S. M. Linear and nonlinear W-cells in C-laminae of the cat's lateral geniculate nucleus. *J. Neurophysiol.* 47: 869-884, 1982.
- TANAKA, K. Cross-correlation analysis of geniculostriate neuronal relationships in cats. *J. Neurophysiol.* 49: 1303-1318, 1983a.
- TANAKA, K. Distinct X- and Y-streams in the cat visual cortex revealed by bicuculline application. *Brain Res.* 265: 143-147, 1983b.
- TANAKA, K. Organization of geniculate inputs to visual cortical cells in the cat. *Vision Res.* 25: 357-364, 1985.
- TOLHURST, D. J. AND DEAN, A. F. Evaluation of a linear model of directional selectivity in simple cells of the cat's striate cortex. *Visual Neurosci.* 6: 421-428, 1991.
- TOYAMA, K., MAEKAWA, K., AND TAKEDA, T. Convergence of retinal inputs onto visual cortical cells. I. A study of the cells monosynaptically excited from the lateral geniculate body. *Brain Res.* 137: 207-220, 1977.
- WILSON, P. D., ROWE, M. H., AND STONE, J. Properties of relay cells in cat's lateral geniculate nucleus: a comparison of W-cells with X- and Y-cells. *J. Neurophysiol.* 39: 1193-1209, 1976.